I. SUPERSATURATION IN HYDROCARBON SYSTEMS

METHANE-n-DECANE

II. SUPERSATURATION IN HYDROCARBON SYSTEMS

METHANE-n-DECANE-SILICA

Thesis by

Franklin Clark Silvey

In Partial Fulfillment of the Requirements

For the Degree of

Chemical Engineer

California Institute of Technology

Pasadena, California

1957

ACKNOWLEDGMENT

I wish to express my gratitude to Professor B. H. Sage for his continued interest and guidance during the course of this research work. The assistance of H. H. Reamer, L. T. Carmichael, W. B. Nichols and W. M. De Witt in obtaining the laboratory measurements and constructing the apparatus is appreciated. The suggestions of Professors W. N. Lacey and W. H. Corcoran who reveiwed the manuscript were very helpful. Virginia Berry and June Gray assisted in preparing the data and illustrations, while Patricia Wilburn did the typing.

During my course of study I received financial aid through an Institute Scholarship and a Graduate Teaching Assistantship. Further assistance, both financial and spiritual, was given by my parents and those of my wife, to whom, in due appreciation, this thesis is dedicated.

ABSTRACT

PART I

An understanding of the possible influence of supersaturated liquids upon the production and refining of petroleum is of industrial interest. Only limited information is available as to the influence of environment upon the duration of supersaturation for pure hydrocarbons and their mixtures.

A number of measurements were made of the influence of strain upon the behavior of four mixtures of methane and n-decane at temperatures ranging from 70° to 390° F. The mixtures exhibited equilibrium bubble-point pressures between 54 and 1048 pounds per square inch. The local strain was introduced by raising the temperature of a portion of the system above that of the remainder.

The formation of bubbles in such systems appears to be randomly distributed in time and its rate is nearly directly proportional to the volume of the phase. The results indicate markedly greater tendency for the persistence of supersaturation than obtained in a pure hydrocarbon but the probability of formation of a bubble under a given condition of strain decreased with an increase in mole fraction methane.

PART II

An understanding of the influence of volume and surface effects upon the duration of supersaturation in hydrocarbon liquids is necessary

to describe the behavior of liquids in a strained state. A very limited amount of information is available on the influence of surface and volume upon supersaturation in pure hydrocarbons.

Preliminary information in this field was obtained using a mixture of methane and n-decane containing 0.2290 mole fraction methane at 220° F. The mixture exhibited an equilibrium bubble-point pressure at 220° F. of 949 pounds per square inch. These measurements were made in equipment in which the strain was introduced by raising the temperature of a portion of the system above that of the remainder.

The volume and surface area of the liquid phase under strain were varied by the introduction of silica crystals. The degree of supersaturation which may be realized in such systems was found to be nearly directly proportional to the volume of the phase. The data were insufficient in number to establish the effect of surface area on bubble formation.

TABLE OF CONTENTS

PART ONE

SUPERSATURATION IN HYDROCARBON SYSTEMS

METHANE-n-DECANE

I. SUPERSATURATION IN HYDROCARBON SYSTEMS

METHANE-n-DECANE

INTRODUCTION

A review of some of the experimental work associated with the supersaturation of hydrocarbon liquids has been made available recently (6). Kennedy and Olson (3) found it possible to maintain hydrocarbon liquids at pressures markedly below bubble-point for short time intervals. In order to extend the data in this field a study of the supersaturation in hydrocarbon liquids was undertaken.

The molecular theory of liquids indicates that significant local fluctuations in the state variables are to be expected at a point as a function of time. These fluctuations result in a wide variation in time during which a system will remain in a strained condition at an invariant macroscopic state. A review of the molecular theory of liquids is contained in Appendix A. Measurements of the time that four mixtures of methane and n-decane could be maintained under different conditions of strain were determined at temperatures ranging from 70° to 390° F. Since the time of strain is random in time, numerous measurements at each condition were required in order to establish the behavior. The standard deviation of the time of strain approaches the mean value as the number of measurements is increased. A regression analysis (6)

was made of the experimental information obtained under each condition of strain for each of the four mixtures. A review of the statistical and regression analysis is given in Appendix B.

MATERIALS

Methane used in this investigation was obtained from the San Joaquin Valley of California. As received at the laboratory it contained approximately 0.001 mole fraction carbon dioxide, 0.0007 mole fraction propane, and 0.0012 mole fraction ethane. The gas was in equilibrium in an aqueous phase at a pressure of approximately 1400 pounds per square inch. The nearly pure methane was passed over calcium chloride, activated charcoal, potassium hydroxide, and anhydrous calcium sulfate at a pressure in excess of 500 pounds per square inch. It was passed through a trap at the temperature of solid carbon dioxide and warmed to room temperature before using. The gas employed did not contain more than 0.002 mole fraction of material other than methane, as established by mass spectrographic analysis.

The n-decane was obtained from Matheson, Coleman and Bell. It was used for these measurements after fractionation at low pressure in a column with 30 plates and deaeration and drying by prolonged refluxing in contact with sodium at reduced pressure. A specific weight at atmospheric pressure of 45.339 pounds per cubic foot at 77° F. was found for the deaerated sample as compared to a value of 45.337 pounds per cubic foot at a temperature of 77° F. reported by Rossini (8). An index of refraction at 77° F. of 1.40974 was obtained for the D-lines of sodium as compared to a value of 1.40967 reported by Rossini (8) for an air-saturated sample.

METHODS AND EQUIPMENT

The method employed in this investigation involved maintaining one relatively small portion of the system at a higher temperature than the remainder, thus localizing the region in which supersaturation occured. The portion of the system at the higher temperature was in a strained condition while the remainder at the lower temperature was maintained at a pressure above the bubble point. Such an arrangement permitted the configutation of the system subjected to strain to be relatively simple, without the existence of liquid-liquid interfaces, packing glands, and other devices which might have a significant influence upon the time-strain relationship of the system.

Figure 1 portrays schematically the nature of the equipment employed. It consists of the pressure vessel A provided with a stainless steel thimble B. The three-stage centrifugal pump C is utilized to circulate the fluid from the entrance of the pump upward through the tube D located at the center of the thimble B. Mercury is introduced or withdrawn from the vessel at E. A multi-lead copper constantan thermocouple is used to determine the temperature of the thimble B relative to the bath H shown in Figure 4, and leads are shown schematically at F and F' in Figure 1. An electric heater G is used to maintain the temperature of the thimble at desired values above that of the pressure vessel A. Details of the pressure vessel A and thimble B are shown in Figure 2.

The mixtures were prepared by the introduction of the desired amount of n-decane and methane by high vacuum techniques. The equilibrium bubble-point pressure was determined for the temperature of interest. A given mixture was often used over a period of several months and it was found that the standard deviation of the bubble-point pressures measured at different times was not more than 0.45 pound per square inch.

To prepare the sample mixture for an experimental test, the system is brought to equilibrium at the bath temperature and is maintained at a pressure of 1000 pounds per square inch above the bubble-point pressure for a specified time, usually several hours. During this time, the centrifugal pump is operated only intermittently. Variations in the time of agitation and of conditioning at high pressure were investigated with one mixture and found not to exert any statistically significant effect on the time of strain. After equilibrium has been obtained throughout the system, the temperature of the thimble is then raised a predetermined amount in order to raise the bubble-point pressure of the portion of the sample within the thimble the desired amount above that of the main body of the liquid. The pressure of the system is then carefully reduced to a value 30 pounds per square inch above the bubble-point pressure of the fluid in the thimble by the withdrawal of mercury. These conditions are maintained for a short period of time to allow the system

to recover from adiabatic cooling effects during the pressure reduction. The pressure is then reduced to a value 5 pounds per square inch above the bubble-point pressure of the main body of liquid by the withdrawal of additional mercury. The situation existing under these circumstances is shown in Figure 3 in which the bubble-point pressure of a methane, n-decane mixture containing 0.2325 mole fraction methane is shown as a function of temperature. The pressure within the vessel is indicated at P and the temperature of the pressure vessel A is maintained at T_A; thus, the state J corresponds to conditions within the vessel A. The temperature of the thimble is shown at T_B corresponding to the equilibrium bubble-point pressure P_b, which being above the pressure in the vessel yields a supersaturated or strained state at K. The magnitude of the supersaturation pressure is given by

$$P_s = P_b - P$$

Such methods are suitable only for mixtures for which the equilibrium bubble-point pressure increases with an increase in temperature.

Figure 4 shows the general layout of the equipment. The various components of the apparatus are interconnected, which permits the exchange of mercury by means of the valve manifolds L and M. Pressure vessel A of Figure 1 is shown within the silicone bath H. The quantity of mercury within the pressure vessel may be controlled by the chamber N

or the mechanical injector Q. Chamber N is utilized for accomplishing approximate pressure changes whereas the injector Q permits accurate pressure changes to be effected. The gauges R indicate the approximate pressure in the vessels A and N. A mercury-oil interface is provided in S so that the pressure can be measured by the balance T (9).

To aid in the control of operations, a transducer U of the strain gauge type and a manostat V (5) are provided to measure pressure as a function of time. A mechanical injector W and chamber X, similar to components Q and N, have been provided for operation in conjunction with the manostat V. The gauges Y permit the determination of the approximate pressure in the manostat V and chamber X. Further description of the details of the equipment has been made available (6).

The temperatures of the agitated silicone baths H and Z are controlled through modulating circuits which have been described (7). The temperatures are related to the international platinum scale by means of a strain-free platinum resistance thermometer (4).

In order to maintain isobaric conditions within the pressure vessel A during an experimental test, a pressure control system is employed. A schematic diagram of the pressure control system is shown in Figure 5. After the initial run pressure in vessel A has been set by balance T of Figure 4, pressure variations may be detected by either the manostat V or transducer U. For the case using the manostat as the pressure

sensing element, variations in pressure are indicated by the displacement of a thin metal diaphragm. A linear transducer in direct contact with the diaphragm, detects any movements of the diaphragm and transmits them as electrical signals to a transducer control unit A_1. When the strain gauge type transducer U is used, the pressure variations are transmitted by the transducer U to a potentiometer B_1. The electrical signals, as received from either the potentiometer or the transducer control unit, determine the position of a galvanometer mirror C_1. An instrument light D_1 is focused on the galvanometer mirror and the position of the mirror varies the amount of light received by the photo-cell E_1. The light shining on the photo-cell controls the output of one of the thyratron power tubes of the modulating circuit F_1. The output of the other thyratron tube can be manually controlled from a separate power supply G_1. The direct current motor H_1 is wired in such a manner as to be run on one direction by the power from J_1 and in the opposite direction by the output of the modulating circuit F_1. Thus, the direct current motor raises or lowers the plunger in the mechanical injector Q and varies the quantity of mercury in pressure vessel A by the correct amount as indicated by the pressure variation signal received by the photo-cell of the modulating circuit F_1.

With the pressure of the system maintained at a constant value, the formation of a bubble is indicated by the requirement for the withdrawal

of mercury to maintain isobaric conditions. The quantity of mercury withdrawn from pressure vessel A is determined by reading the revolution counter located on the drive shaft of the mechanical injector Q. In order to determine the bubble formation time accurately, a continual record of the quantity of mercury in pressure vessel A as a function of time is necessary. In order to facilitate equipment operation, the volume-time relationship is automatically recorded by a data processing unit. The data processing unit was designed and constructed by L. T. Carmichael and is shown diagramatically in Figure 6.

In the time standard section of the data processing unit, a 60 cycle synchronous motor K_1 is mechanically connected to a selsyn L_1 and a timer cam M_1. The revolutions of the synchronous motor, one per second, are transmitted electrically by the selsyn L_1 through a terminal board N_1, and a differential selsyn P_1 to a secondary selsyn Q_1. Mechanically connected to the secondary selsyn are: a visual readout counter R_1, a 10 to 1 gear reduction box S_1, and a magnetic brake T_1. The gear reduction box steps down the shaft speed to meet the requirements of the digitizer U_1. The digitizer is an electro-mechanical device which converts the rotating shaft positions into decimal form and actuates the electric printer V_1. A bank of four micro-switches W_1, utilizing a 1-1/2 volt direct current power source X_1, are mounted in direct contact with the timer cam M_1. One of the micro-switches sends an impulse to

the preset counter Y_1 every second. The preset counter counts the pulses and when the desired number have been accounted for, closes an internal relay which activates the magnetic brake T_1, from a 30 volt direct current power source Z_1, and fixes the position of the visual readout counter R_1 and the digitizer U_1. After the brake has been energized, a second micro-switch actuates the power pack A_2. The power pack provides the necessary voltages and interlocks to cause the electric printer V_1 to print digital information from the digitizer U_1 when energized from a push button or remote actuator. When the electric printer has recorded the desired information on a continuous paper tape, a third micro-switch releases the magnetic brake T_1. With the magnetic brake released, the differential selsyn P_1 resets the secondary selsyn Q_1 to correspond to the position of the synchronous motor K_1. Should the electric printer fail to clear itself in the printing operation, a fourth micro-switch actuates an alarm bell B_2 which rings every second until the trouble is remedied. The electric printer can be forced to print and clear itself by actuating the power pack A_2 a second time from its push button.

In the volume recording section of the data processing unit, most of the components are the same as for the time standard section. The direct current motor H_1 drives the mechanical injector Q of Figure 5 and determines the position of the visual readout counter C_2. The shaft

speed to the mechanical injector can be selected by a gear box D_2. A selsyn E_2 transmits the position of the visual readout counter C_2 through the terminal board N_1 and differential selsyn F_2 to a secondary selsyn G_2 and visual readout counter H_2. Mechanically connected to the visual readout counter H_2 are: a 10 to 1 gear reduction box J_2, a magnetic brake K_2, and a digitizer L_2; the digitizer being connected to the electric printer V_1. Thus, the volume of mercury contained in the pressure vessel A of Figure 1 may be automatically recorded at any desired time interval.

An auxiliary selsyn M_2, mechanically connected to an electric motor N_2, may be connected through the terminal board N_1 to the visual readout counter and digitizer assembly of either the time standard or volume recording sections of the data processing unit. This combination is used to set these assemblies to any desired position.

A schematic diagram of the circuit employed in controlling the temperature of the stainless steel thimble B is shown in Figure 7. This circuit is similar to one which has been described (7) for the temperature control of silicone baths. The multi-lead thermocouple, shown schematically at F and F', serves the function of both a measuring and controlling element. The actual temperature is determined from the reading of the potentiometer P_2 by a direct experimental calibration against a strain-free platinum resistance thermometer (4). The function of the galvanometer

mirror Q_2, instrument light R_2, and photo-cell S_2, is the same as has been described for the pressure control system in Figure 5. A modulating circuit T_2 provides the power to heater G required to maintain the desired temperature in the thimble B.

EXPERIMENTAL RESULTS

Typical results for a mixture of methane and n-decane containing 0.0355 mole fraction methane at a stress of 29.68 pounds per square inch are shown in Figure 8. The bubble-point pressure at equilibrium for 160° F. was 120 pounds per square inch. The sample was maintained under nearly isobaric-isothermal conditions throughout the period of strain. The times of strain for a particular set of conditions of stress were obtained from a series of experimental measurements such as the one depicted in Figure 8. A summary of the experimental results obtained with four mixtures of methane and n-decane at temperatures ranging from 70° to 390° F. is recorded in Table I. During the period when these measurements were made it was not feasible to hold the temperature of the system at systematically chosen values, which would have been desirable.

Utilizing the data of Table I, there is shown in Figure 9 for a mixture containing 0.2765 mole fraction methane, the probability of a bubble not being formed under one experimental condition of strain as a function of time. The volume, area, and temperature indicated refer only to that portion of the system under strain. The mixture had an equilibrium bubble-point pressure of 1048 pounds per square inch and was subjected to a stress of approximately 97.6 pounds per square inch. The primary variable, $P(0,\theta)$, of the ordinate of Figure 9 was determined

from the difference between unity and the ratio of the number of trials with supersaturation times less than that of, but including, the trial in question to the total number of trials plus one (1). Such an evaluation of the probability involves some uncertainty, but affords a simple means of processing the experimental data. A straight line (2) was fitted to the data of Figure 9 by the method of least squares. The slope of such a line for each of the conditions of supersaturation investigated is included in Table II. The value of the slope computed from the mean time is also recorded along with the standard deviation of the times of strain from the mean time. These data indicate that the formation of a bubble in a fixed total volume is random with respect to time (10) as was predicted from the theory of liquids and found experimentally for pure propane (2) and pure n-pentane (6).

The time of strain is shown in Figure 10 as a function of the supersaturation pressure for the same mixture of 0.2765 mole fraction methane. Again the volume, area, and temperature refer only to that portion of the system under strain. There is a decrease in the time of strain with an increase in stress. This trend is apparent despite more than a tenfold variation in the time of strain at a fixed stress. The same information is presented in Figure 11 except it has been assumed that the Arrhenius relation describes the effect of supersaturation upon the time of strain (2, 6). The curve drawn on Figure 10 was fitted by

least squares methods whereas that of Figure 11 was fitted by a regression analysis. The standard deviation in time for the data shown was 8311 seconds for Figure 10 and 7548 seconds in Figure 11.

Utilizing the data of Table I, the probability of a bubble forming (6) as a function of time for a given degree of strain is shown in Figures 12 and 13 for a total volume of liquid phase of 0.000411 cubic foot. The confidence limits of these data are rather poor as is shown in Table II. Wide disagreements from the predictions are to be encountered for a particular trial. In Figure 12 for a mixture containing 0.0120 mole fraction methane at 354.5° F. a probability of bubble formation of 0.71 at 20,000 seconds at a stress of 9.41 pounds per square inch is indicated. Stresses of 112.5 pounds per square inch may be realized within an equal probability for nearly 40,000 seconds in the case of a mixture containing 0.2325 mole fraction methane at 267.9° F. The higher probability of bubble formation shown at short times for the supersaturation of 101.5 pounds per square inch as compared to the behavior at 112.5 pounds per square inch is not believed to be significant.

In order to present some of the trends of the data, the probability of bubble formation is depicted in Figure 14 for three rather widely different conditions. Within the confidence limits of the data all three conditions yield the same probability of bubble formation at a given time. The supersaturation pressure necessary to yield a given time for the

formation of a bubble is shown in Figure 15 as a function of the mole fraction methane. The effect of temperature upon this behavior was not considered here although it may prove to be important in the light of more extensive investigations. The information presently available does not indicate temperature to be of great importance. Figure 15 indicates a trend toward much higher supersaturation pressure for a given time before bubble formation as the mole fraction methane is increased in the methane, n-decane system.

A rather extensive investigation of variations in the time of agitation and of conditioning over pressure during the procedure followed in preparing a sample for an experimental test was made with a mixture containing 0.0355 mole fraction methane. The effect on the time-strain relationship of the system was made at an average stress of approximately 30.24 pounds per square inch. The results of the investigation are recorded in Table III. Utilizing the data of Table III, there is shown in Figure 16 the time for bubble formation as a function of conditioning time for three different agitation periods. Since a similar distribution of bubble formation times is obtained for each agitation time at various conditioning times, no significant statistical effect can be attributed to the length of the conditioning period.

REFERENCES

1. Gumbel, E. J., "Statistical Theory of Extreme Values and Some Practical Applications," U. S. Department of Commerce, Natl. Bur. Standards, Applied Math. Series, 33, Washington, D. C., 1954.

2. Hunt, E. B., Jr., and Berry, V. J., Jr., Am. Inst Chem. Engrs. Journal, 2, 560 (1956).

3. Kennedy, H. T., and Olson, C. R., Trans. Am. Inst. Mining Met. Engrs., 195, 271 (1952).

4. Meyers, C. H., Natl. Bur. Standards J. of Research, 9, 807 (1932).

5. Nichols, W. B., Ph. D. Thesis, California Institute of Technology, Pasadena, 1957.

6. Nichols, W. B., Carmichael, L. T., and Sage, B. H., "Supersaturation in Hydrocarbon Systems. n-Pentane in the Liquid Phase," accepted for publication in Ind. Eng. Chem.

7. Reamer, H. H., and Sage, B. H., Rev. Sci. Instr., 24, 46 (1945).

8. Rossini, F. D., et al., "Selected Values of the Physical and Thermodynamic Properties of Hydrocarbons and Related Compounds," Carnegie Press, Pittsburgh, 1953.

9. Sage, B. H., and Lacey, W. N., Trans. Am. Inst. Mining Met. Engrs., 136, 136 (1940).

10. Wilks, S. S., "Mathematical Statistics," Princeton University Press, Princeton, 1943.

NOMENCLATURE

ℓn	natural logarithm
n_1	mole fraction methane
P	pressure, lb./sq.in.
$\mathcal{P}$	probability of a bubble being formed
P_b	bubble-point pressure, lb./sq.in.
P_s	supersaturation pressure ($P_b - P$), lb./sq.in.
θ_b	time of strain to first bubble, sec.
θ_c	conditioning time, min.
$\bar{\theta}_m$	mean time corresponding to a given value of supersaturation pressure, sec.

Superscript

*	time average of quantity during run

LIST OF TABLES

TABLE I. SUMMARY OF EXPERIMENTAL RESULTS FOR MIXTURES OF METHANE AND n-DECANE IN HEATED THIMBLE EQUIPMENT

Identification	Number of Experimental Points	Supersaturation Pressure Lb./Sq.In.	Standard Deviation Lb./Sq.In.	Bubble Formation Time Sec.	Rate of Bubble Formation Bubbles/(Sec.)(Cu.Ft.)	Thimble Temperature °F.
Mole Fraction Methane = 0.2765 Average Thimble Temperature = 77.7°F.						
19484	1	115.13[a]	0	395	6.161	88.98
19493	3	115.18	0	2098	0.785	89.06
21103	2	119.34	0.71	2156	1.128	87.72
21107	10	119.97	0.32	4714	0.516	88.00
21115	1	119.88	0	387	6.285	88.31
21120	8	120.00	0.35	4245	0.573	88.17
21124	10	119.89	0	2766	0.880	88.13
21129	6	119.50	0.52	753	3.231	87.86
21137	5	120.63	1.10	1178	0.265	88.56
21142	4	119.83	0	1870	1.301	88.10
21147	1	119.79	0	318	7.651	88.23
21152	10	119.79	0	3908	0.623	87.84
21156	7	119.95	0.38	2095	1.161	88.16
21161	6	119.31	0.55	1246	1.953	87.86
21165	6	120.81	0	1392	1.748	88.51
21184	10	97.47	1.41	13050	0.186	78.87
21189	3	98.81	0	855	2.846	79.02
21193	11	98.81	0	4837	0.503	78.92
21199	7	98.80	0	5375	0.453	79.06
21204	12	102.05	0.58	8006	0.304	79.14
21209	21	101.66	1.60	10714	0.227	79.23
21221	19	89.35	6.19	11687	0.208	75.22
21238	6	90.48	2.61	4384	0.555	75.09
21248	2	83.20	0.96	1315	1.850	70.73

[a] Average supersaturation pressure
[b] 10-minute agitation time
[c] 25-minute agitation time
[d] 100-minute agitation time

TABLE I (Cont.)

Identification	Number of Experimental Points	Supersaturation Pressure Lb./Sq.In.	Standard Deviation Lb./Sq.In.	Bubble Formation Time Sec.	Rate of Bubble Formation Bubbles/(Sec.)(Cu.Ft.)	Thimble Temperature °F.
		Mole Fraction Methane = 0.2765 Average Thimble Temperature = 77.7°F.				
21253	7	80.32	2.70	5810	0.419	70.93
21264	1	79.78	0	238	10.225	70.71
21269	64	79.50	2.34	43295	0.056	71.05
21216	19	92.11	3.19	12354	0.197	74.99
21280	4	79.76	0	937	2.597	71.00
21285	4	78.77	1.10	1225	1.986	70.71
21297	9	72.42	1.81	5391	0.451	68.07
21302	9	74.67	0.15	7055	0.345	68.06
21318	39	71.75	4.13	21437	0.113	68.14
21325	24	75.67	3.75	11932	0.204	70.78
		Mole Fraction Methane = 0.2325 Average Thimble Temperature = 273.1°F.				
19291	8	124.42[a]	0.38	5963	0.408	287.21
19295	8	101.46	2.23	9503	0.256	252.22
19300	63	91.34	2.69	84508	0.029	243.61
19304	48	102.20	5.02	65923	0.037	251.92
19320	1	124.80	0	328	7.418	288.78
19324	82	105.78	5.06	83111	0.029	256.60
19328	38	115.08	1.89	33327	0.073	267.67
19332	12	124.35	0.52	1595	1.526	287.08
19336	17	113.60	3.48	13754	0.177	268.02
19340	12	123.42	2.45	6579	0.370	287.54
19344	4	112.64	3.20	1623	1.499	267.97
19348	4	129.36	0.75	892	2.732	308.48
19352	12	129.45	0.17	1702	1.430	308.76
19360	17	129.08	2.21	4614	0.527	309.58
19364	57	115.20	2.78	64356	0.038	268.05
19368	4	105.42	0.77	1627	1.495	257.07

TABLE I (Cont.)

Identification	Number of Experimental Points	Supersaturation Pressure Lb./Sq.In.	Standard Deviation Lb./Sq.In.	Bubble Formation Time Sec.	Rate of Bubble Formation Bubbles/(Sec.)(Cu.Ft.)	Thimble Temperature °F.
		Mole Fraction Methane = 0.2325 Average Thimble Temperature = 273.1°F.				
19372	10	102.24	4.98	6027	0.404	257.17
19376	7	123.21	3.07	3475	0.700	287.41
19385	7	129.44	0.14	1122	2.169	308.42
19389	16	101.25	1.49	12782	0.190	252.54
19393	2	129.74	0	972	2.503	310.66
19397	18	100.19	2.52	13252	0.184	252.76
		Mole Fraction Methane = 0.0120 Average Thimble Temperature = 359.3°F.				
19149	3	8.25[a]	0.06	2589	0.940	350.07
19153	2	17.89	0.06	153	15.898	386.97
19161	2	17.32	0.01	202	12.048	385.19
19165	14	6.76	0.75	12985	0.187	353.01
19169	3	15.01	0	405	6.006	377.16
19173	15	6.45	0.57	17652	0.138	343.34
19177	28	6.87	0.64	34011	0.072	342.46
19185	4	9.48	0.07	4548	0.535	355.53
19190	2	14.76	0.01	174	13.986	376.62
19194	22	9.53	0.51	46889	0.052	355.55
19198	2	14.70	0.06	398	6.112	376.36
19202	1	9.27	0	589	4.131	354.80
19207	5	9.44	0.08	10705	0.227	355.60
19215	10	9.48	0.94	17229	0.141	355.58
		Mole Fraction Methane = 0.0355 Average Thimble Temperature = 311.0°F.				
21408	1	30.55[a, b]	-	295	8.248	328.29
21417	3	29.63	0.14	3058	0.796	306.96
21422	27	29.65	2.04	51056	0.048	307.03
21427	12	29.68	1.22	20068	0.121	307.09
21432	5	29.39	0.60	6265	0.388	307.19

TABLE I (Cont.)

Identification	Number of Experimental Points	Supersaturation Pressure Lb./Sq.In.	Standard Deviation Lb./Sq.In.	Bubble Formation Time Sec.	Rate of Bubble Formation Bubbles/(Sec.)(Cu.Ft.)	Thimble Temperature °F.
Mole Fraction Methane = 0.0355 Average Thimble Temperature = 311.0°F.						
21437	11	29.54	2.47	19847	0.123	307.10
21447	9	29.82	0	15270	0.159	307.04
21453	54	29.76	1.17	108731	0.022	307.02
21458	6	28.53	3.63	7583	0.321	307.30
21463	40	29.72	1.22	92207	0.026	306.99
21476	37	29.66	2.44	30876	0.079	307.14
21481	28	31.95	1.34	52884	0.046	314.10
21486	4	30.88	0.66	1214	2.004	314.08
21495	31	30.82	1.71	27892	0.087	314.08
21500	5	30.25	1.55	793	3.068	314.00
21527	6	30.98[c]	1.03	2964	0.821	313.97
21533	3	30.03	1.87	661	3.681	314.04
21538	4	31.32	0.41	1976	1.231	314.24
21543	11	31.57	1.77	14830	0.164	314.12
21558	12	30.23	2.17	7579	0.321	311.15
21563	10	30.49	1.14	10970	0.222	311.29
21568	15	30.10	1.30	15605	0.156	311.10
21574	24	30.50	1.90	23059	0.106	311.04
21588	11	31.29	1.26	7441	0.327	310.93
21593	10	30.24	1.42	7373	0.330	310.94
21598	6	30.88	0.62	3366	0.723	311.13
22408	20	31.01	1.92	19670	0.124	310.99
22418	9	28.93	3.90	5459	0.446	311.14
22423	8	28.88	2.94	3509	0.693	311.23
22443	8	28.89	2.21	2443	0.996	310.97
22458	8	30.24	1.53	5223	0.466	311.06
22487	18	30.42	0.29	19965	0.122	311.08
22506	7	28.69	3.21	4498	0.541	311.19
22530	3	29.22	1.86	565	4.306	310.79
22547	52	30.33	1.70	56030	0.043	310.07
22618	46	31.27	1.14	77199	0.032	311.07
22636	39	31.62	0.71	67059	0.036	311.16

TABLE I (Cont.)

Identification	Number of Experimental Points	Supersaturation Pressure Lb./Sq.In.	Standard Deviation Lb./Sq.In.	Bubble Formation Time Sec.	Rate of Bubble Formation Bubbles/(Sec.)(Cu.Ft.)	Thimble Temperature °F.
		Mole Fraction Methane = 0.0355 Average Thimble Temperature = 311.0°F.				
22517	37	30.48[d]	1.53	39541	0.062	311.43
22537	2	29.90	1.19	1098	2.216	311.00
22600	5	30.69	0.41	5361	0.454	311.25
22606	25	29.96	1.24	39487	0.062	311.09
22642	40	31.36	0.65	63397	0.038	311.03
22648	2	30.42	0.71	2089	1.165	311.12
22654	39	31.26	0.89	56700	0.043	311.01

TABLE II. COMPARISON OF PREDICTED AND EXPERIMENTAL STANDARD DEVIATIONS

Average Thimble Temperature °F.	Composition Mole Fraction Methane	Number of Points	Supersaturation Pressure Lb./Sq. In.	Mean Time to First Bubble Sec.	Standard Deviation[a] Sec.	Rate of Bubble Formation Bubbles/(Sec.)(Cu. Ft.)	
88.2	0.2765	15	119.5[b]	2017	1430	1.206	1.319[c]
77.7	0.2765	9	97.59	7787	4274	0.312	0.341
70.0	0.2765	10	77.85	9164	14036	0.265	0.411
298.4	0.2325	10	127.0	2509	1942	0.971	0.988
267.9	0.2325	4	112.5	26696	23632	0.091	0.110
253.0	0.2325	8	101.5	32431	43351	0.075	0.096
380.5	0.0120	5	15.62	263	95	9.246	9.903
354.5	0.0120	6	9.21	16097	21537	0.151	0.235
342.9	0.0120	3	6.67	25128	19924	0.097	0.139
310.4	0.0355	15	29.99[d]	29179	33571	0.083	0.093
311.6	0.0355	22	30.32[e]	16247	21794	0.149	0.117
311.1	0.0355	7	30.58[f]	29750	26552	0.082	0.070

[a] Deviation from mean time
[b] Reference supersaturation pressure
[c] Least squares
[d] 10-minute agitation time
[e] 25-minute agitation time
[f] 100-minute agitation time

TABLE III. SUMMARY OF THE EFFECT OF CONDITIONING AND AGITATION ON BUBBLE FORMATION

Identification	Conditioning Time, Min.	Agitation Time, Min.	Bubble Formation Time, Sec.
	Mole Fraction Methane = 0.0355 Average Thimble Temperature = 311.0°F.		
21491	21	10	125
21505	23	10	79
21509	29	10	82
21412	33	10	6768*
21522	38	10	55
21495	39	10	27892
21408	55	10	295
21437	72	10	19847
21476	82	10	30876
21463	85	10	92207
21432	87	10	6265
21453	87	10	108731
21427	94	10	20068
21481	111	10	52884
21500	112	10	793
21486	128	10	1214
21447	143	10	15270
21548	144	10	7538
21422	152	10	51056
21417	172	10	3058
22482	12	25	52
22477	15	25	51
22524	20	25	182
22618	22	25	77199
22530	24	25	565
22595	27	25	58963*
22547	29	25	56030

TABLE III (Cont.)

Identification	Conditioning Time Min.	Agitation Time Min.	Bubble Formation Time Sec.
	Mole Fraction Methane = 0.0355 Average Thimble Temperature = 311° F.		
22561	30	25	123337*
22418	45	25	5459
21558	48	25	7579
22408	48	25	19670
22636	50	25	67059
22404	67	25	57
21538	68	25	1976
21574	70	25	23059
22443	79	25	2443
22423	89	25	3509
21533	90	25	661
22453	91	25	136
21588	93	25	7441
22487	94	25	19965
22458	95	25	5223
21568	111	25	15605
21553	120	25	189
21563	125	25	10970
21593	125	25	7373
21527	129	25	2964
21598	144	25	3366
21543	149	25	14830
22579	278	25	134210*
22642	11	100	63397
22648	14	100	2089
22438	14	100	123
22612	15	100	136738*
22606	20	100	39487
22654	21	100	56700
22626	23	100	144909*
22449	24	100	88

TABLE III (Cont.)

Identification	Conditioning Time	Agitation Time	Bubble Formation Time
	Min.	Min.	Sec.
	Mole Fraction Methane = 0.0355 Average Thimble Temperature = 311.0° F.		
22433	28	100	125
22464	31	100	44
22493	34	100	30
22469	41	100	70
22600	159	100	5361
22511	977	100	164
22517	1115	100	39541
22568	1125	100	165
22555	1127	100	75600*
22537	1185	100	1098
22586	1318	100	64558*

* Test discontinued before formation of bubble.

LIST OF FIGURES

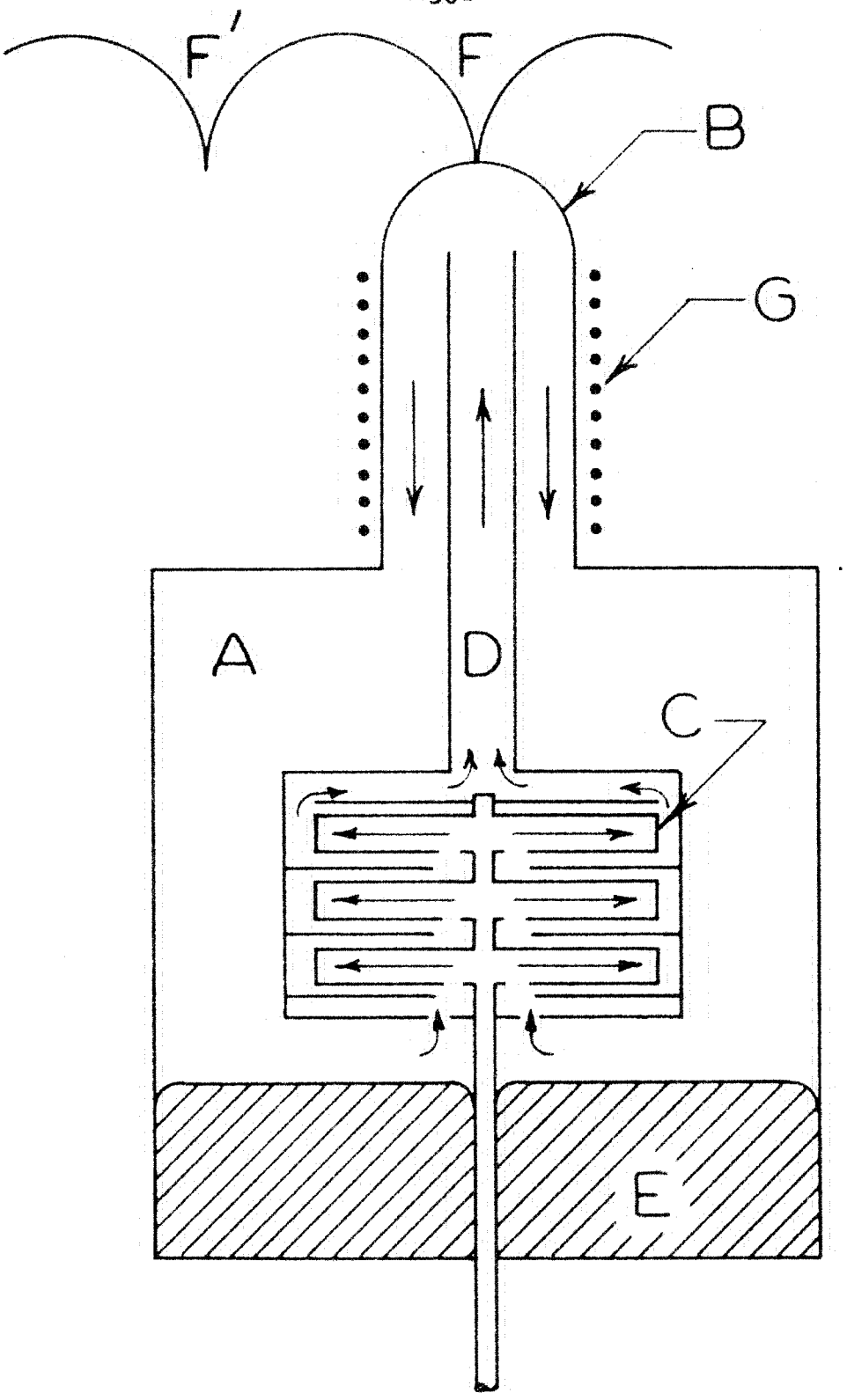

Fig. 1. Schematic Arrangement of Equipment

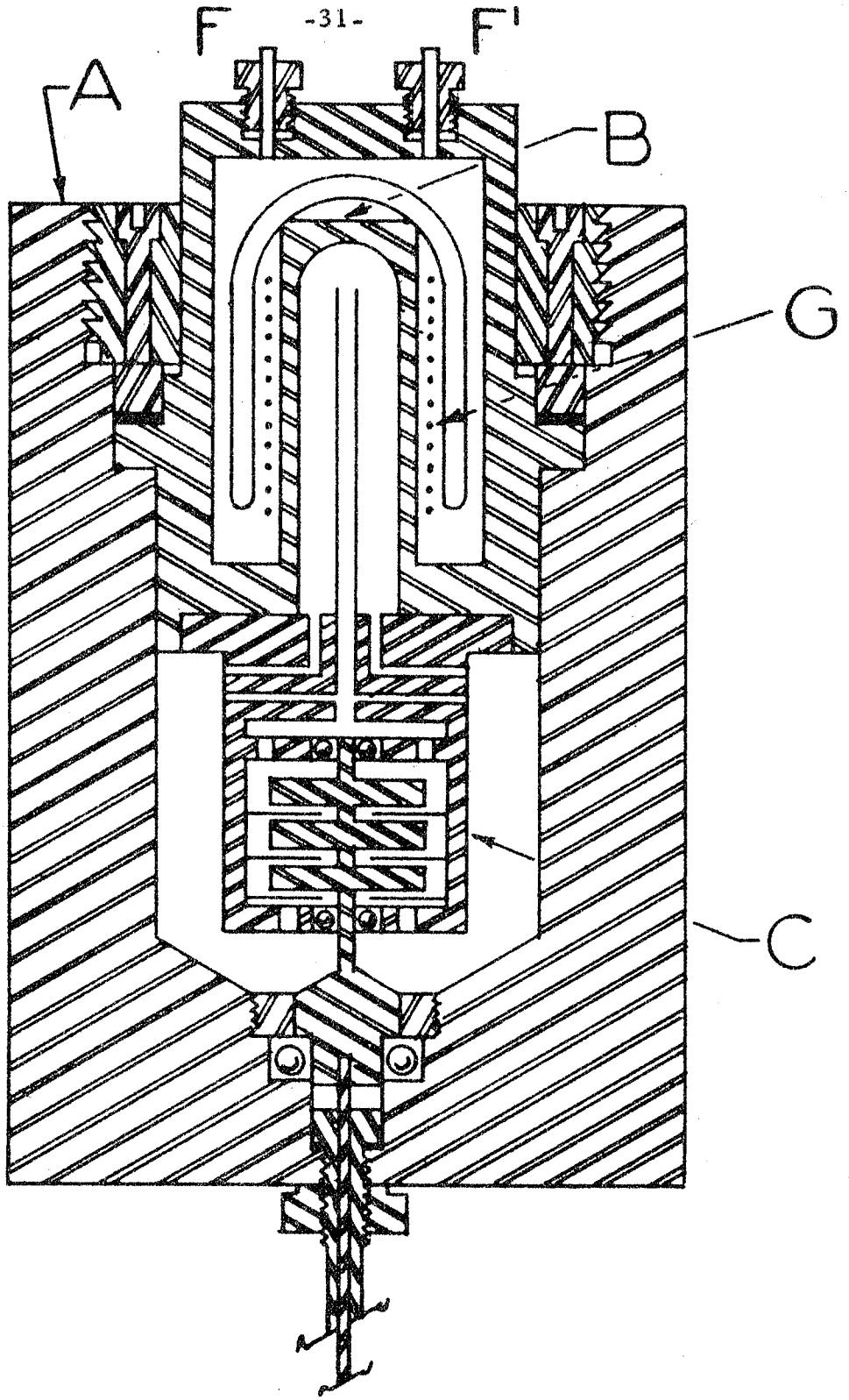

Fig. 2. Sectional View of Pressure Vessel

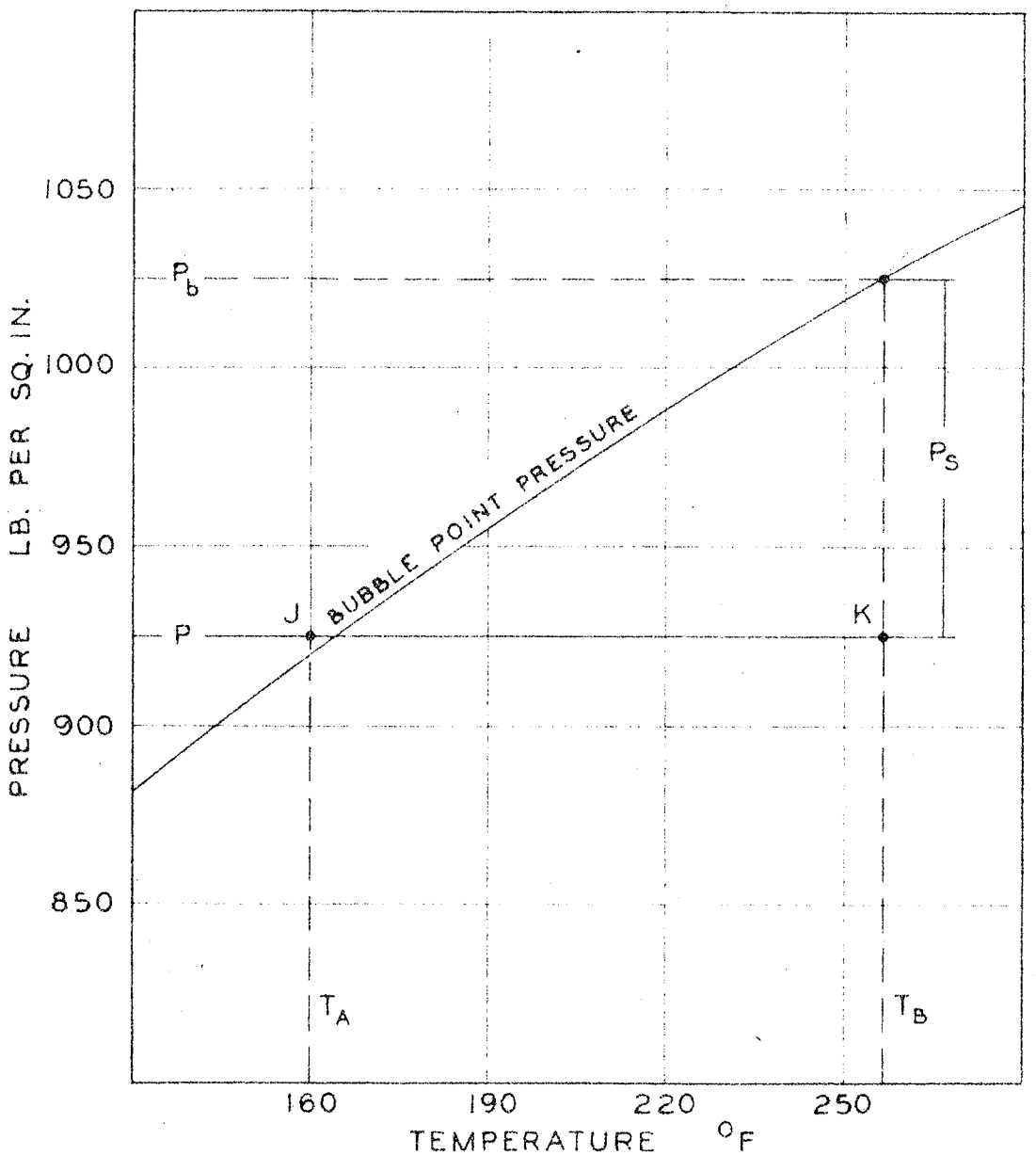

Fig. 3. Pressure-Temperature Diagram for a Mixture Containing 0.2325 Mole Fraction Methane

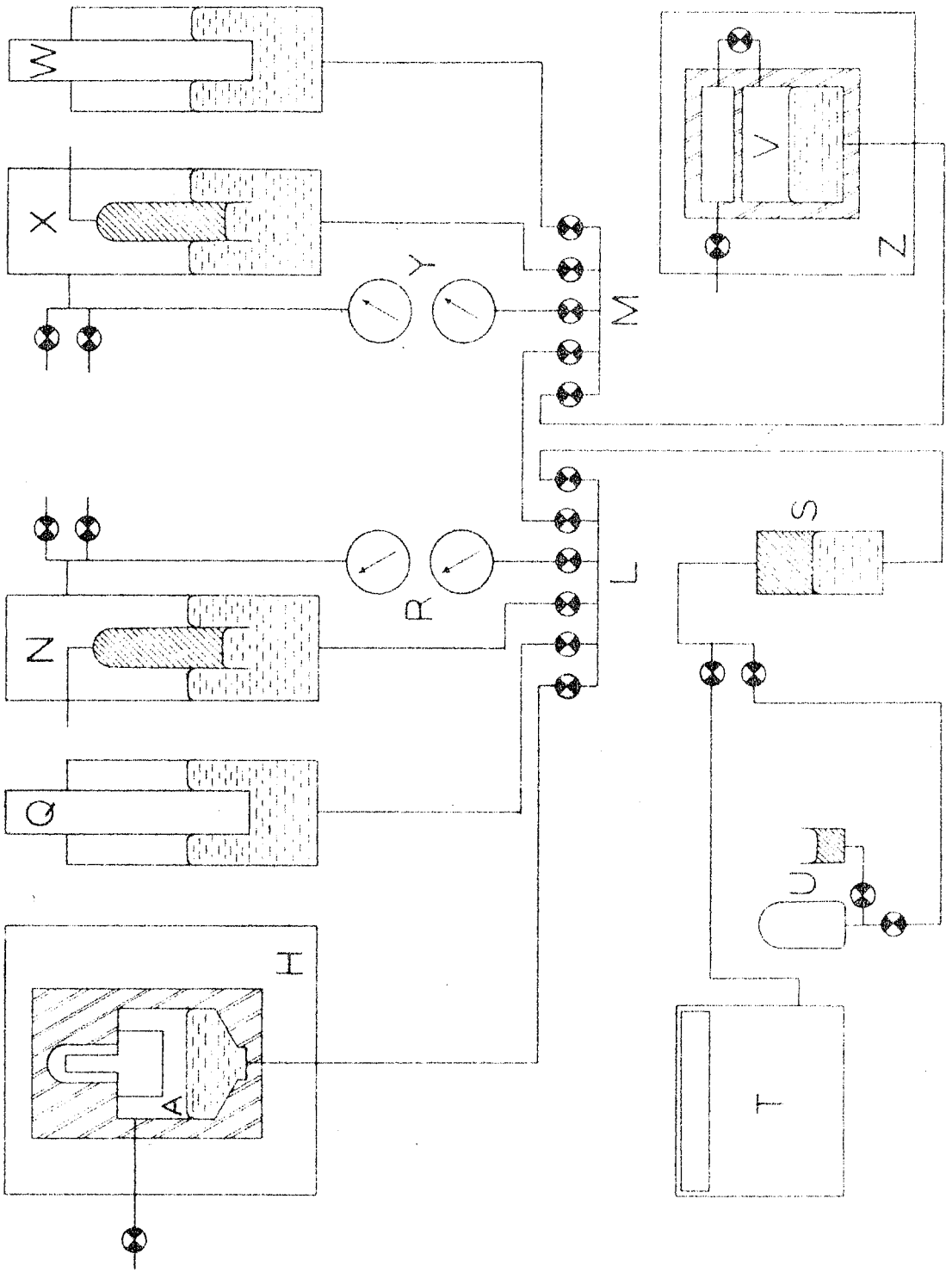

Fig. 4. Arrangement of Associated Equipment

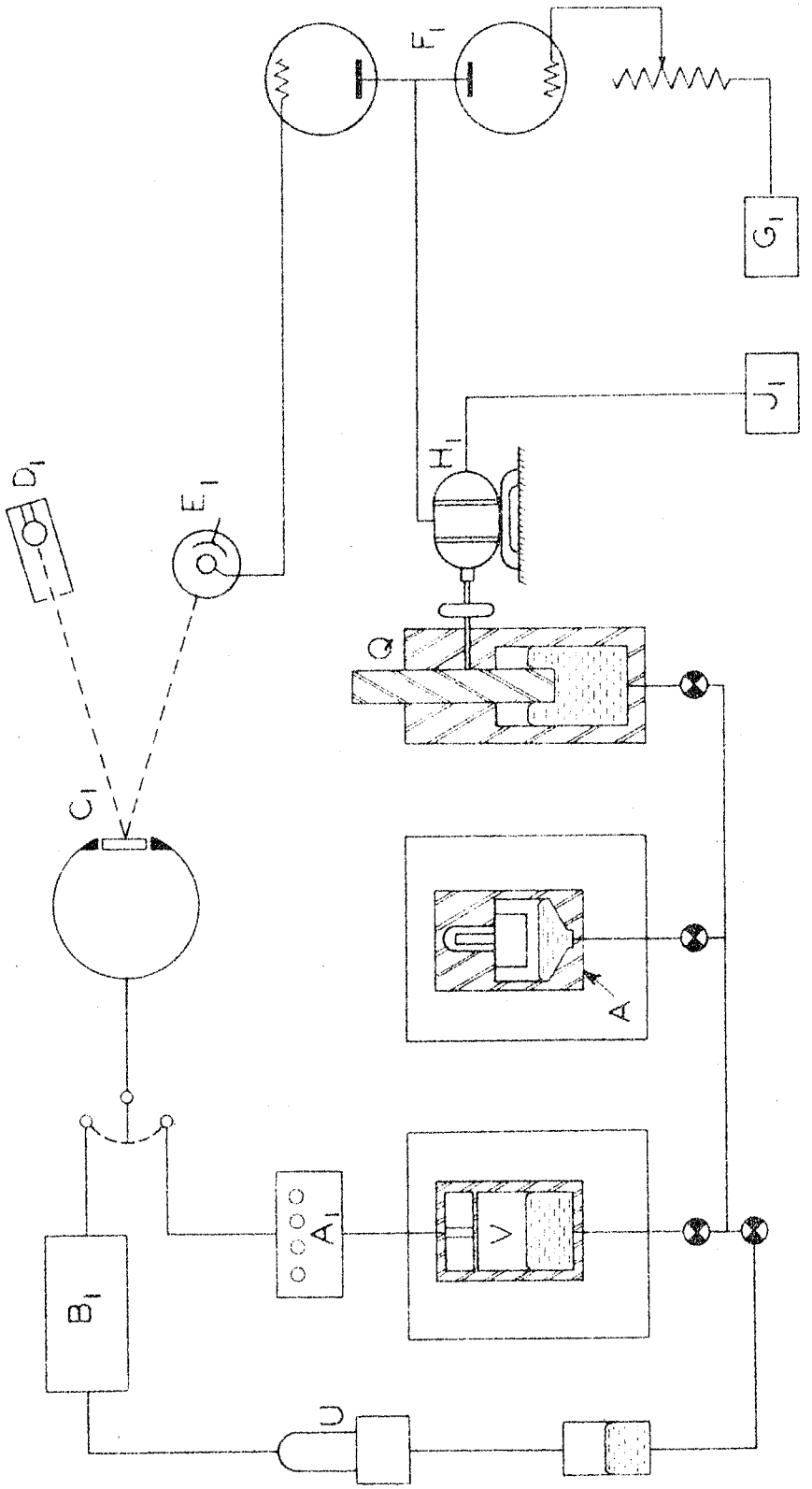

Fig. 5. Schematic Diagram of Pressure Control System

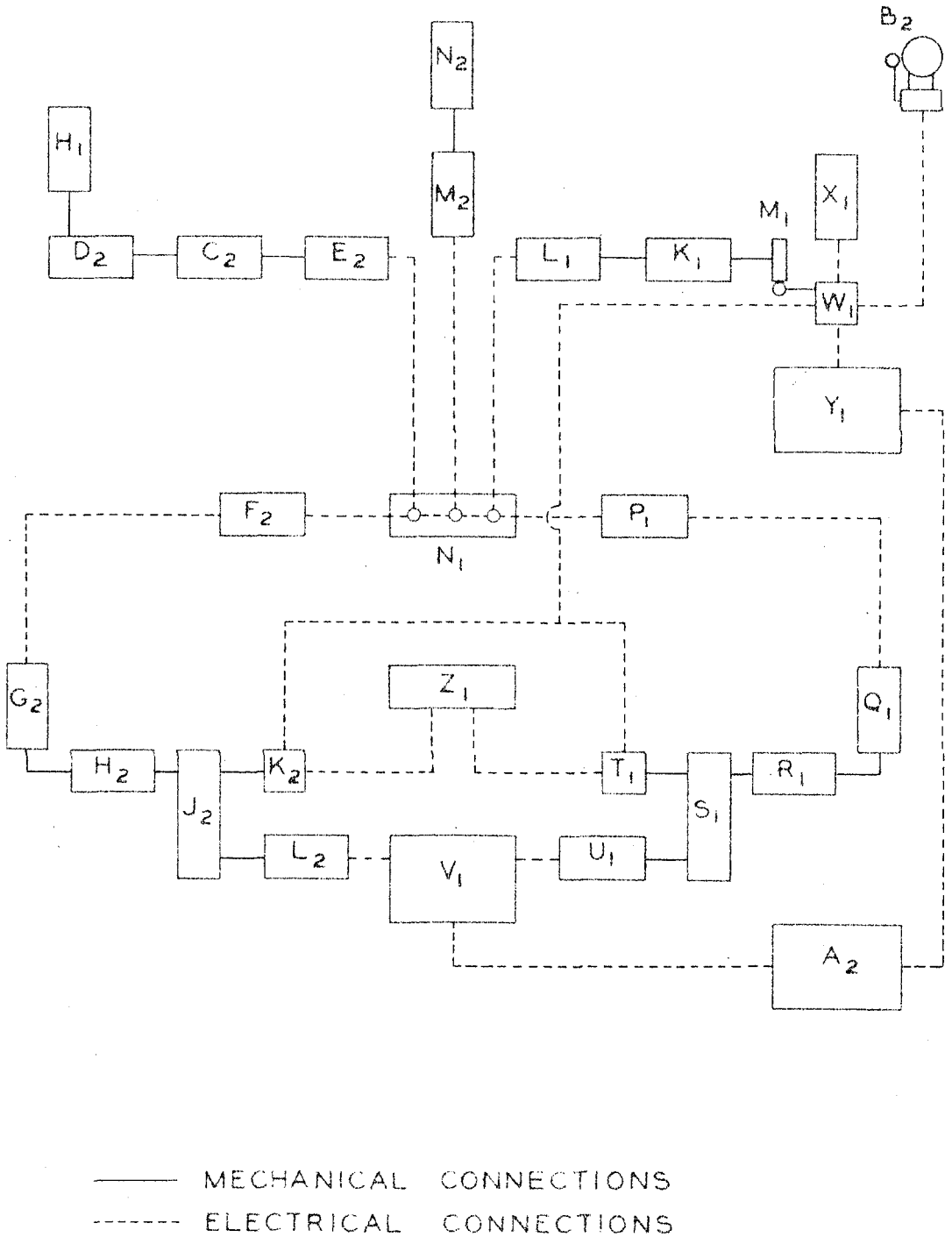

Fig. 6. Schematic Diagram of Data Processing Unit

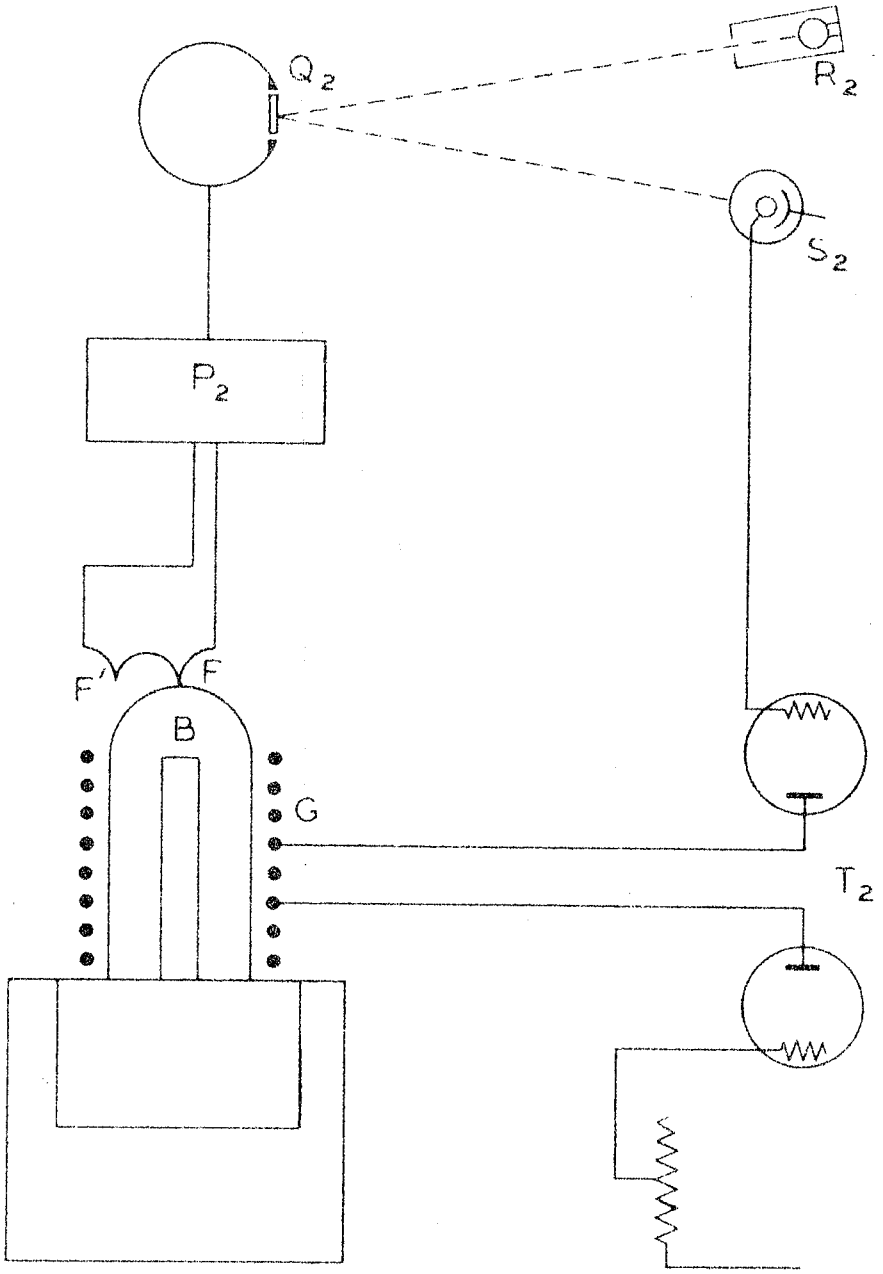

Fig. 7. Schematic Diagram of Thimble Temperature Control System

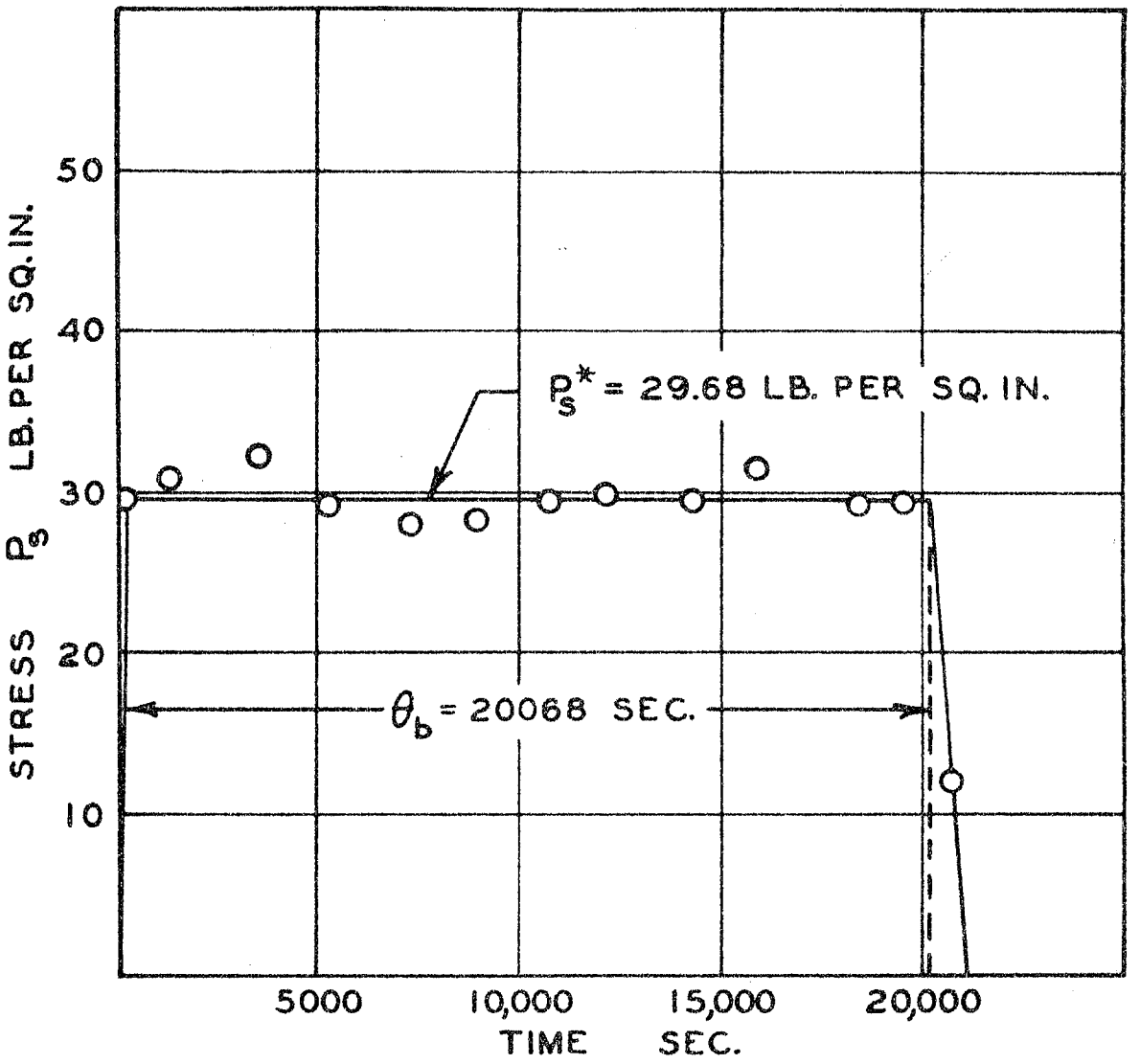

Fig. 8. Typical Experimental Results for a Mixture Containing 0.0355 Mole Fraction Methane

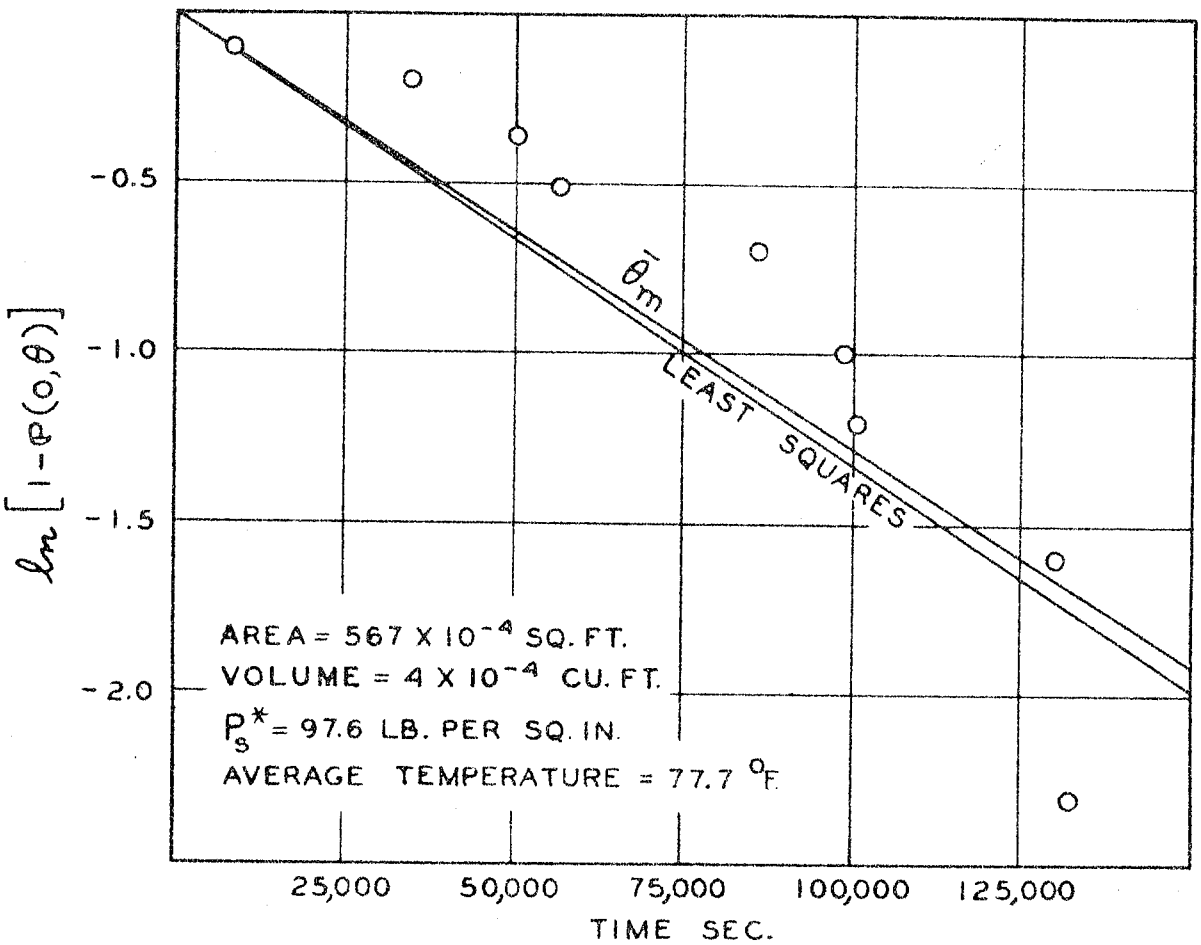

Fig. 9. Probability of a Bubble Not Being Formed in a Mixture Containing 0.2765 Mole Fraction Methane

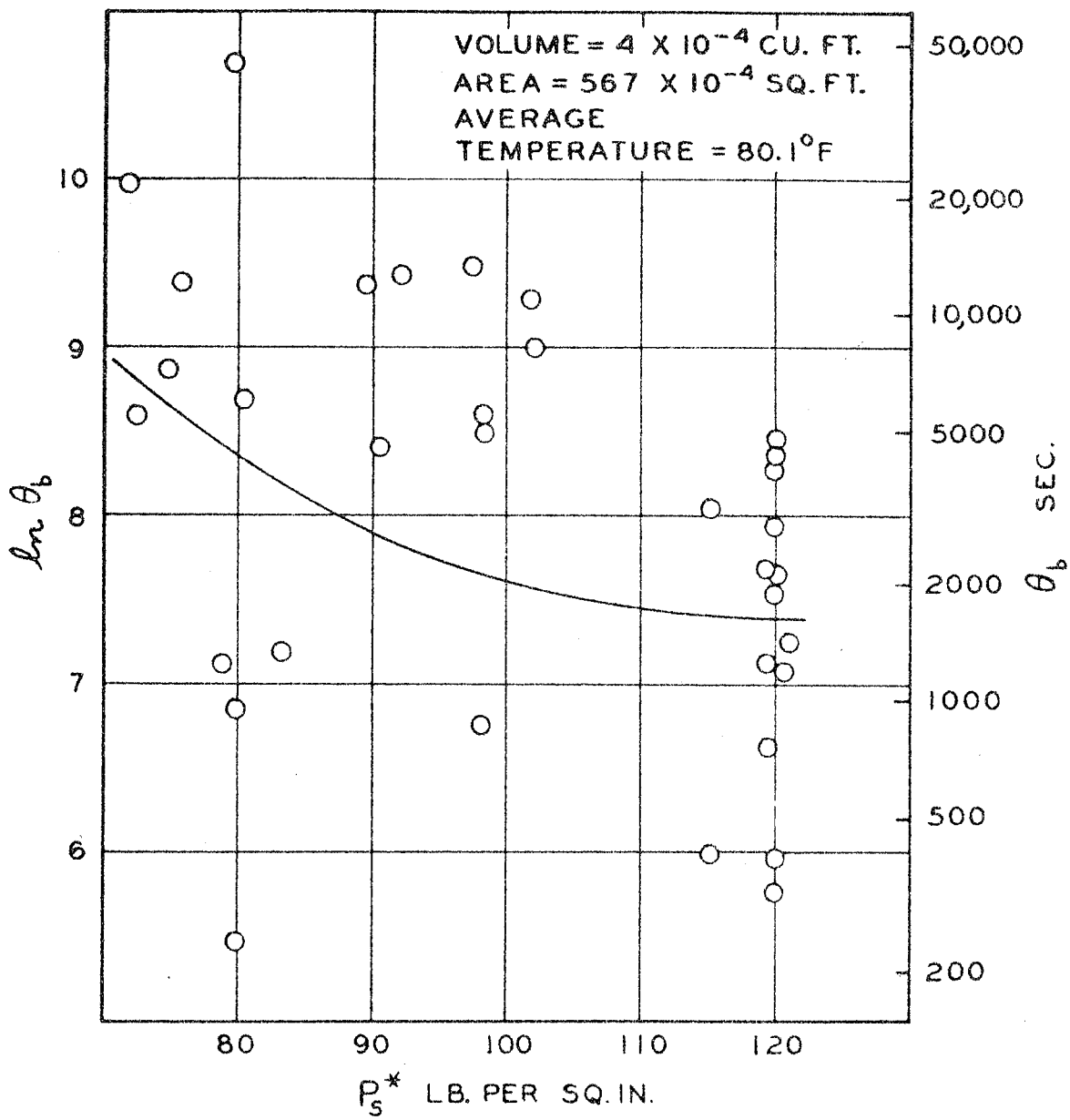

Fig. 10. Effect of Stress on Time of Strain for a Mixture Containing 0.2765 Mole Fraction Methane

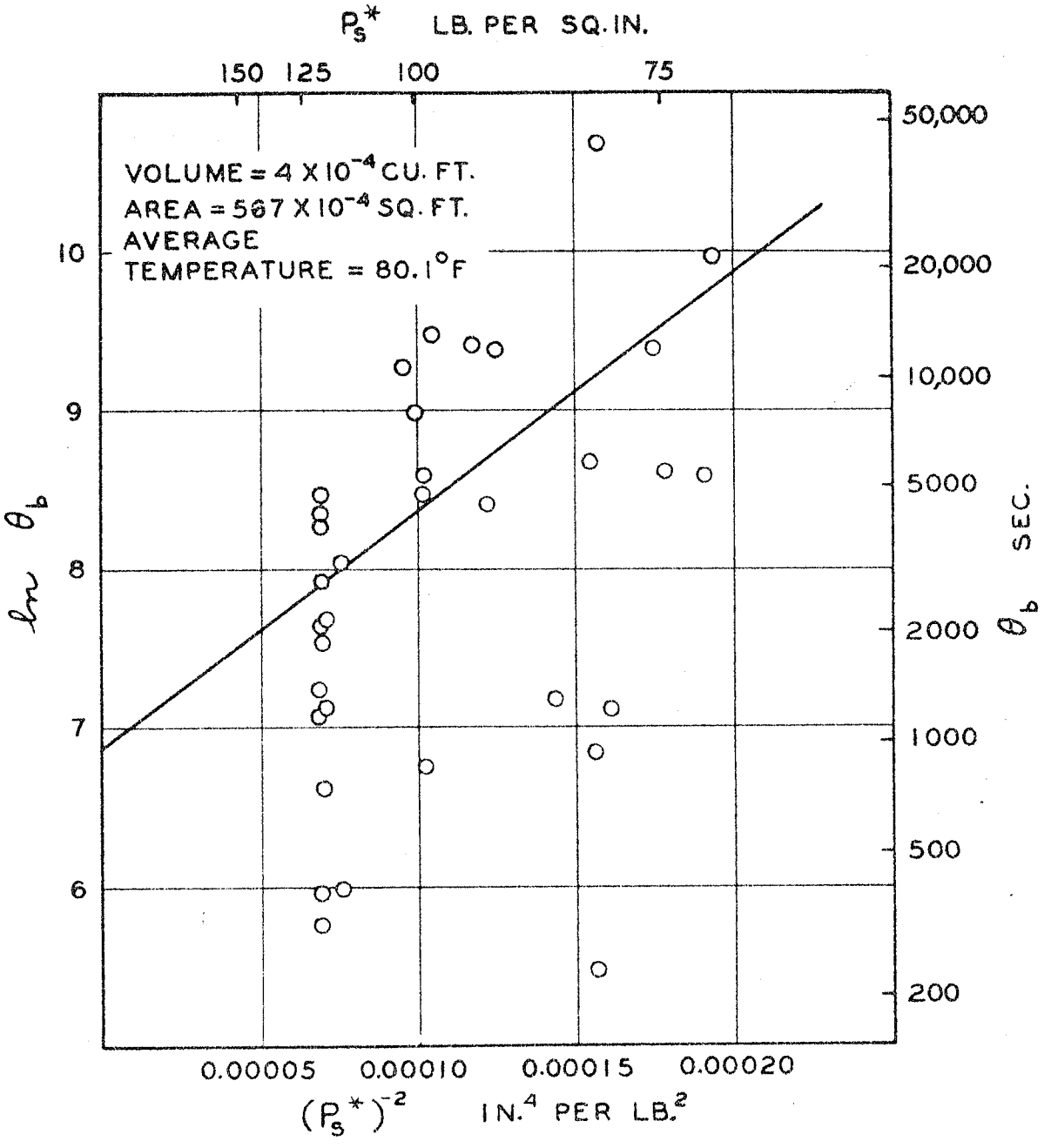

Fig. 11. Application of Arrhenius Relation to Behavior of Mixture Containing 0.2765 Mole Fraction Methane

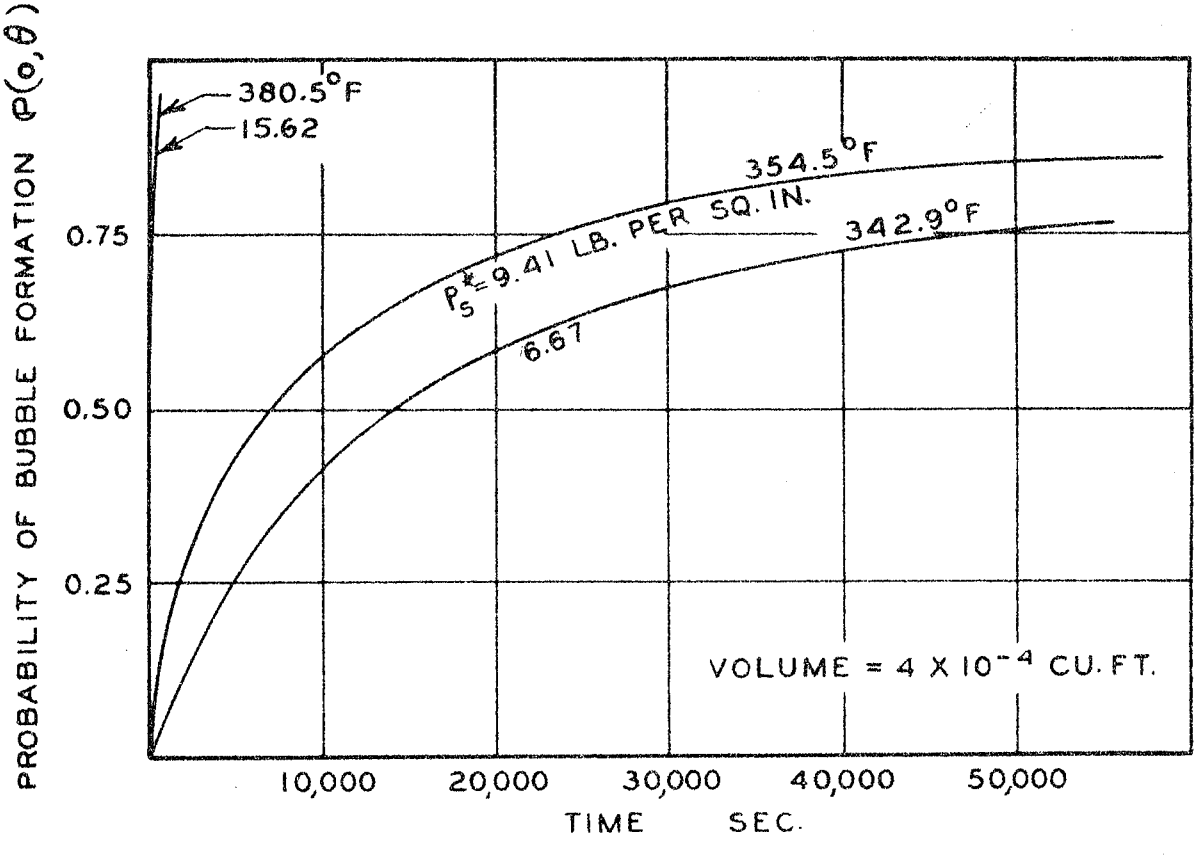

Fig. 12. Probability of Bubble Formation for a Mixture Containing 0.0120 Mole Fraction Methane

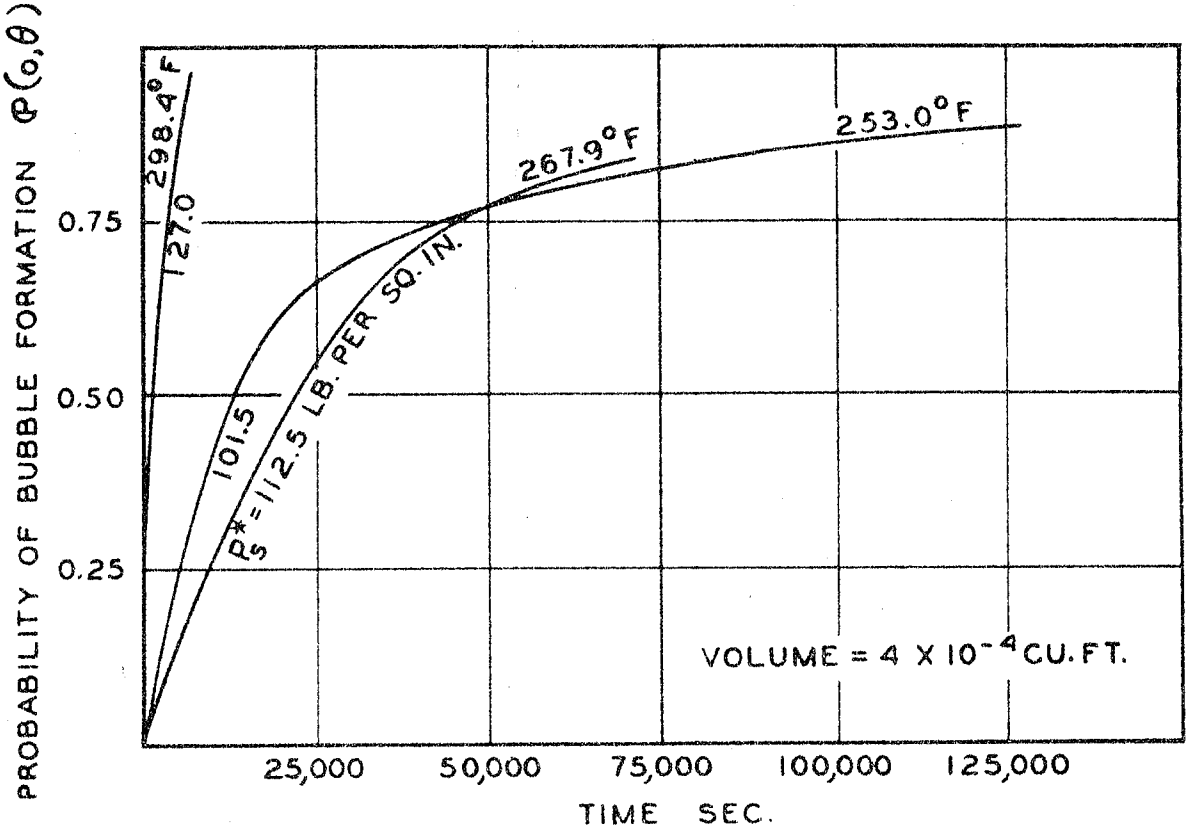

Fig. 13. Probability of Bubble Formation for a Mixture Containing 0.2325 Mole Fraction Methane

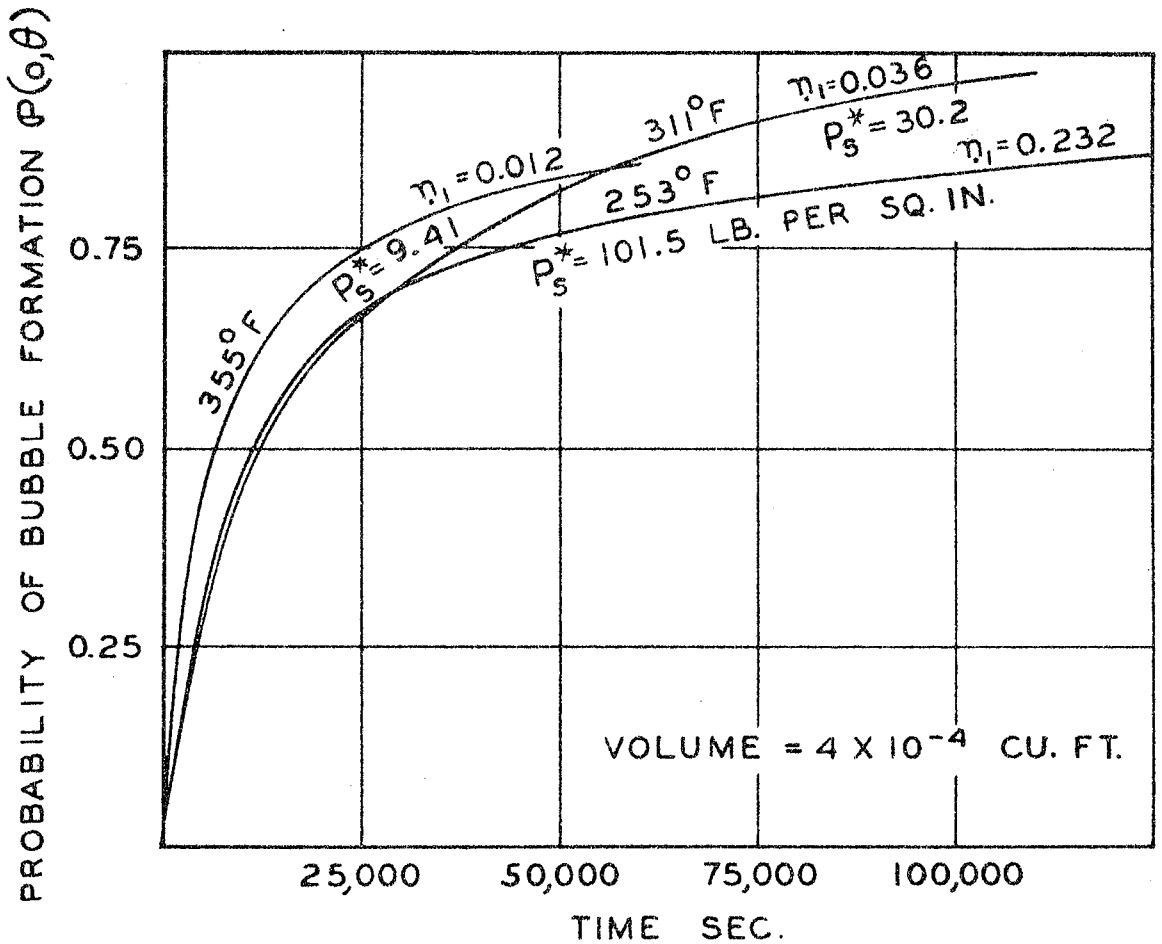

Fig. 14. Trends in Probability of Bubble Formation

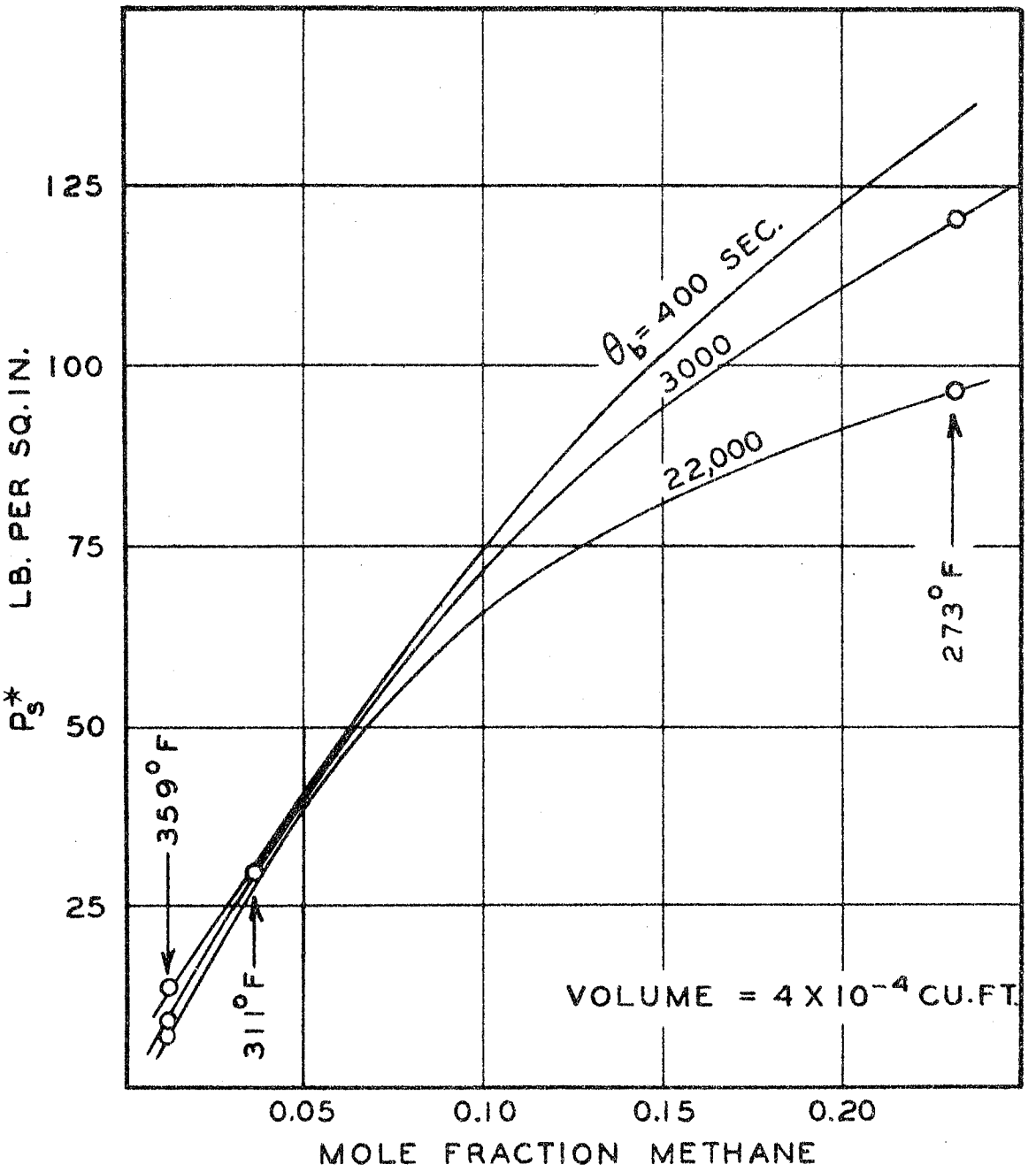

Fig. 15. Possible Effect of Composition upon Supersaturation Pressure

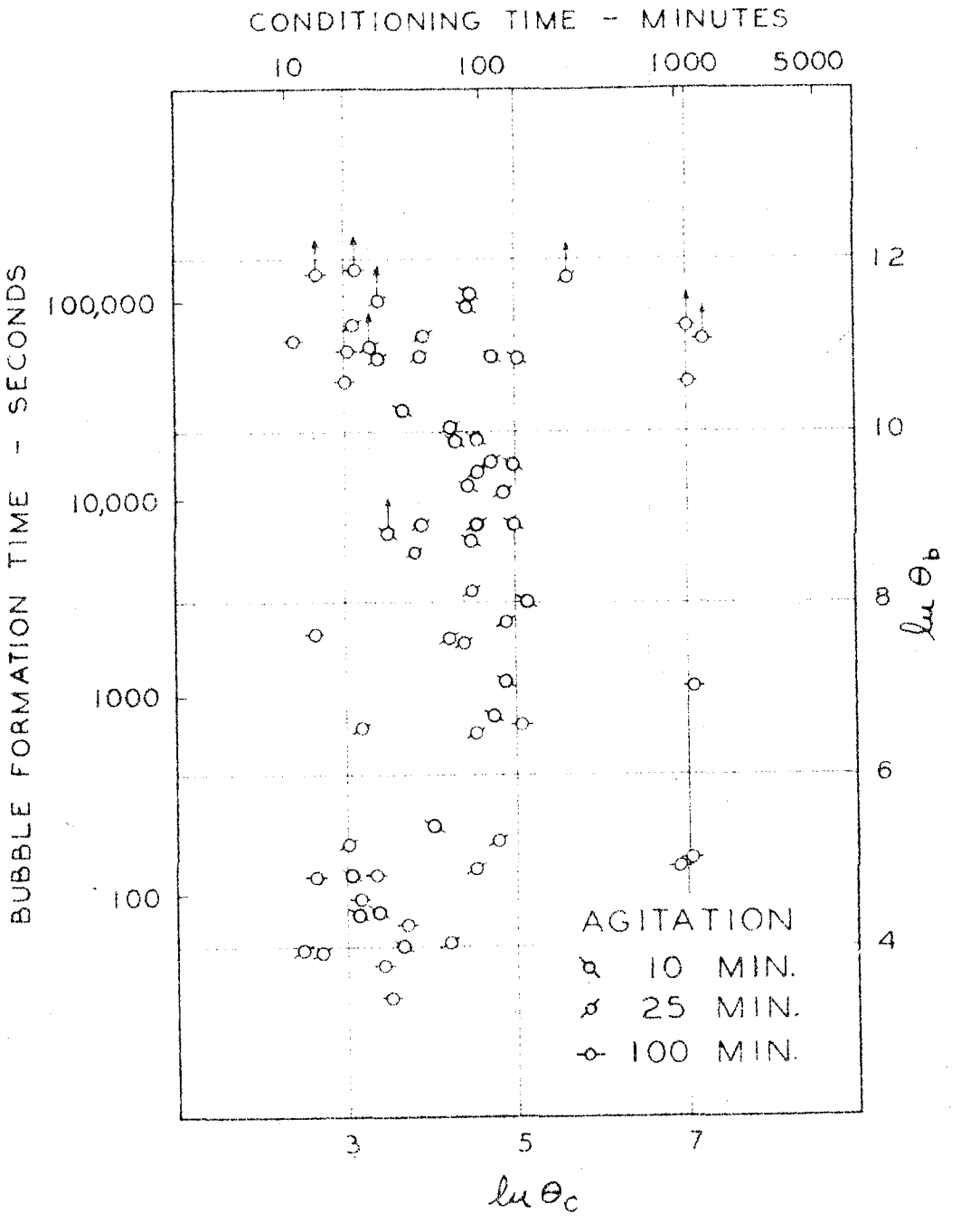

Fig. 16. Effect of Conditioning on Duration of Supersaturation

PART TWO

SUPERSATURATION IN HYDROCARBON SYSTEMS

METHANE-n-DECANE-SILICA

II. SUPERSATURATION IN HYDROCARBON SYSTEMS

METHANE-n-DECANE-SILICA

INTRODUCTION

Only a very limited number of data are available on the effect of sample volume and surface area in contact with a liquid phase on the duration of supersaturation. Recently, the influence of volume and total surface area was investigated for pure n-pentane (2). The heated thimble apparatus, described in Part I of this thesis, and a spherical isochoric vessel (3) were used to study the time-strain relationship for n-pentane at 160° F. The data obtained with the isochoric equipment involved nearly 21 times the volume of n-pentane and nearly 4 times the surface area that was employed in the heated thimble equipment. Each set of measurements was corrected to a unit volume basis and after making this correction, there was little to choose in a statistical sense between the experimental data from the two pieces of equipment. However, the data were insufficient in number to establish the effect of surface area on bubble formation.

The influence of solid surfaces upon the duration of a given degree of supersaturation in water containing dissolved carbon dioxide was investigated by Marboe and Weyl (1). The ability of various materials with different surface characteristics to release bubbles from the

solutions of carbon dioxide in water was studied from a qualitative standpoint.

In order to extend the data on the influence of volume and surface, a study of the supersaturation in mixtures of methane and n-decane containing silica crystals was undertaken.

MATERIALS

The methane and n-decane used in this investigation have been previously described in Part I of this thesis. The silica crystals were obtained from Mr. John Sherborne of the Union Oil Company of California. These crystals had been sized by standard screens so that the largest crystal would pass a 48 mech screen and the smallest crystals were retained on a 150 mesh screen. Hence, the approximate size range of the crystals is 0.0058 to 0.0116 inch. Prior to their use, the silica crystals were immersed in pure n-pentane for a period of one hour to remove the surface impurities and then dried thoroughly.

METHODS AND EQUIPMENT

The method employed in this investigation has been previously described in Part I of this thesis. Only three changes in the method of operation and equipment were made.

The stainless steel thimble B and tube D shown on Figure 1 were filled with silica crystals. Figure 2 shows the crystals magnified 23 times and provides an illustration of their size distribution, while Figure 3, which shows three crystals of different size magnified 70 times, furnishes an indication of their shapes. The crystals are held in place by two stainless steel supports, A and C, to which two layers of 120 mesh stainless steel wire cloth were soldered. Dry compressed air was employed to transport the crystals into the thimble and tube. When the thimble and tube were filled with silica, the porosity of this section of the apparatus was 39.2 per cent and the volume available for a sample was 0.000161 cubic foot. From the enlarged view of the crystals shown in Figure 2, an average dimension for a representative crystal was found to be 0.0083 inch. Assuming the shape of the crystal to be cubic, a first approximation of the total surface area, based on the average dimension calculated from Figure 2, was determined. The surface area under these restrictions was found to be 1.325 square feet. Thus, the addition of the silica crystals to the thimble B and tube D has decreased the volume 60.8 per cent and increased the total

surface area 23.4 times.

In preparing a sample for an experimental test, the same procedure as has been previously described was employed with two modifications. The speed of the pump, utilized to circulate the sample through the thimble, was increased about 25 per cent to 1300 revolutions per minute and the time of agitation was increased to 60 minutes. These changes, necessary to compensate for the increased resistance to flow because of the presence of the silica crystals, were effected to establish more complete mixing throughout the entire sample.

The pressure control system, previously described in Part I of this thesis, was not employed as such in these measurements. Instead, the system when under stress was allowed to "float" on the manostat. In this operation, the large gas volume contained in the manostat effectively absorbed the major fluctuations in pressure and maintained the pressure within 0.2 pound per square inch. Since the volume of mercury in the pressure vessel remains constant throughout the experimental test, the formation of a bubble is indicated by a continued rise in pressure. In order to afford a continuous record of pressure in the system as a function of time, a Speedomax recorder was used. An illustration of a typical pressure-time chart produced by the Speedomax is shown in Figure 4. The dashed portion of the curve represents the time, during the beginning of an experimental test, before the manostat

is connected to the system. The record of the Speedomax starts at the point E and continues to the end of the test. The formation of a bubble is indicated by the pressure rise at the point F.

EXPERIMENTAL RESULTS

A summary of the experimental results obtained with a mixture of methane and n-decane containing 0.2290 mole fraction methane at a temperature of 220° F. is recorded in Table I. The bubble-point pressure at equilibrium for 220° F. was 949 pounds per square inch.

Utilizing the data of Table I and similar information for a mixture containing 0.2325 mole fraction methane which was investigated at 273.1° F. in Part I of this thesis, there is shown in Figure 5 the effect of total sample volume upon the duration of supersaturation. For both of the mixtures studied, the distribution of times for bubble formation over the range of stresses studied is essentially the same, however, the range of supersaturation pressures is markedly different. The curves of Figure 5 were fitted by least squares methods. For the mixture containing 0.2325 mole fraction methane, the total volume of liquid phase under stress was 0.000411 cubic foot, while the total volume of the sample containing 0.2290 mole fraction methane was reduced to 0.000161 cubic foot due to the presence of silica crystals. For the case when the thimble is partially filled with the silica crystals, the average time for bubble formation for a stress of approximately 25.4 pounds per square inch would be 2000 seconds. In the absence of the crystals, the same average time for bubble formation would be realized for a strain of about 126.1 pounds per square inch. Similarly, an

average bubble formation time of 20,000 seconds would be realized for stresses of approximately 98.9 pounds per square inch for a total volume of 0.000411 cubic foot and 19.1 pounds per square inch in a total volume of 0.000161 cubic foot. Thus, by decreasing the total volume of liquid phase under strain approximately 60.8 per cent, the degree of supersaturation which may be realized for an equal length of time is reduced about 80 per cent.

The effect of the presence of the silica crystals on the time for bubble formation can be shown by extrapolating the curves shown on Figure 4 to equal value of strain. The results, at best, are only approximate but give a good illustration of the dependence of the time-strain relationships for the system upon surface area and volume. When extrapolated to a stress of 60 pounds per square inch, the mixture containing 0.2290 mole fraction methane in a volume of 0.000161 cubic foot would have an average time for bubble formation of about 38 seconds. In a like manner, for a mixture containing 0.2325 mole fraction methane, the average bubble formation time is approximately 1.86×10^7 seconds. Using the average times obtained by extending the data, the bubble formation rates, corrected to a unit volume basis, for the mixtures containing 0.2290 and 0.2325 mole fraction methane are 163.0 and 0.000131 bubbles/(sec.)(cu. ft.) respectively.

The presence of the silica crystals greatly increases the total

surface area in contact with the volume of sample under strain. A rough estimate of the total surface area showed it had been increased approximately 23.4 times. Undoubtedly the increase in the surface area has a marked effect on the time-strain relationship of the system, however, until a more exact measurement of the total surface area of the crystals is obtained, this effect cannot be fully explained. An indication of the possible effect of surface area upon bubble formation may be seen from the data in Table II. Here, the rates of bubble formation in the two mixtures under comparison have been corrected to a unit volume basis. After making this correction there still exist large differences in the rates, which suggests that the effect of the change in total surface area must be considered. However, further experimental study will be necessary to establish whether the effect of surface area or total volume has the more pronounced influence on the behavior.

Utilizing the data of Table I, the probability of a bubble forming (2) as a function of time for a given degree of strain is shown in Figure 6 for a total volume of liquid phase of 0.000161 cubic foot. For comparison, the stresses of 127.0 and 112.5 pounds per square inch as shown on Figure 13 of Part I for a mixture containing 0.2325 mole fraction methane and a total volume of 0.000411 cubic foot are included in Figure 6. The confidence limits of these data are rather poor as is

shown in Table II. Wide disagreements are to be encountered for a particular trial. Here again the influence of volume on bubble formation is emphasized as, within the confidence limits of the data, stresses of 112.5 pounds per square inch in the case of a liquid phase volume of 0.000411 cubic foot and 19.1 pounds per square inch for a volume of 0.000161 cubic foot may be realized with equal probability for 60,000 seconds. Similarly, under essentially the same conditions, for stresses of 127.0 and 28.3 pounds per square inch respectively, the probability of bubble formation is the same for at least 5000 seconds. A regression analysis (2) of the data for the mixture containing 0.2290 mole fraction methane was not undertaken at this time as the experimental studies with this mixture has been only partially completed. As a result, the stresses reported for this composition in Figure 6 were averaged values rather than reference supersaturation pressures.

CONCLUSIONS AND RECOMMENDATIONS

The preliminary results obtained with a mixture of methane and n-decane containing 0.2290 mole fraction methane have shown the marked effect of variations in volume and surface area on the duration of supersaturation. The measurements with this mixture should be continued to establish the time-strain behavior of the system at 220° F. more completely.

Since it appears that changes in volume and surface area are of major importance, these effects should be investigated as thoroughly as those of composition and temperature. The data as shown in Figure 4 could be expanded by using larger silica crystals in the thimble at the same temperature and composition. This would add considerably to the information presently available, and determine the advisability of continuing investigations in this field.

To differentiate between the relative importance of volume or surface area effects, the possibility of filling the thimble with small stainless steel spheres should be considered. Here, the variations in volume and surface area as recommended for the silica crystals could be simulated and, in addition, the effect of the presence of a smooth surface in contact with the liquid phase under strain could be compared with the sharp, angular surface of the silica crystals.

REFERENCES

1. Marboe, E. C., and Weyl, W. A., J. Soc. Glass Technol., 32, 281 (T) (1948).

2. Nichols, W. B., Carmichael, L. T., and Sage, B. H., "Supersaturation in Hydrocarbon Systems. n-Pentane in the Liquid Phase," accepted for publication in Ind. Eng. Chem.

3. Reamer, H. H., and Sage, B. H., Rev. Sci. Instr., 24, 46 (1945).

NOMENCLATURE

n_1	mole fraction methane
P	pressure, lb./sq.in.
P_b	bubble-point pressure, lb./sq.in.
P_s	supersaturation pressure ($P_b - P$), lb./sq.in.
$\mathcal{P}$	probability of a bubble being formed
T	temperature, ^oF.
V	volume of liquid phase under strain, cu.ft.
θ_b	time of strain to first bubble, sec.

Superscript

*	time average of quantity during run

LIST OF TABLES

TABLE I. SUMMARY OF EXPERIMENTAL RESULTS FOR A MIXTURE OF METHANE AND n-DECANE IN HEATED THIMBLE APPARATUS HAVING A VOLUME OF 0.000161 CUBIC FOOT

Identification	Number of Experimental Points	Average Supersaturation Pressure Lb./Sq.In.	Standard Deviation Lb./Sq.In.	Bubble Formation Time Sec.	Thimble Temperature °F.
		Mole Fraction Methane = 0.2290 Average Thimble Temperature = 220.0°F.			
22805	9	20.40	0.77	28669	220.04
22828	18	18.76	0.47	63995	220.07
22842	9	18.82	0.54	22459	220.02
22849	3	18.27	0.74	8864	219.86
22861	3	28.06	1.93	1724	219.96
22868	2	27.70	3.44	483	220.00
22882	4	29.10	1.12	1165	220.07

TABLE II. COMPARISON OF BUBBLE FORMATION RATES

Average Thimble Temperature °F.	Composition Mole Fraction Methane	Number of Points	Supersaturation Pressure Lb./Sq.In.	Mean Time to First Bubble Sec.	Standard Deviation Sec.	Rate of Bubble Formation Bubbles/(Sec.)(Cu.Ft.)
220.0	0.2290	4	19.1[a]	30997	23502[b]	0.201
220.0	0.2290	3	28.3	791	743	7.86
267.9	0.2325	4	112.5	26695	23632	0.091
298.4	0.2325	10	127.0	2509	1942	0.971

[a] Reference or average supersaturation
[b] Deviation from mean time

LIST OF FIGURES

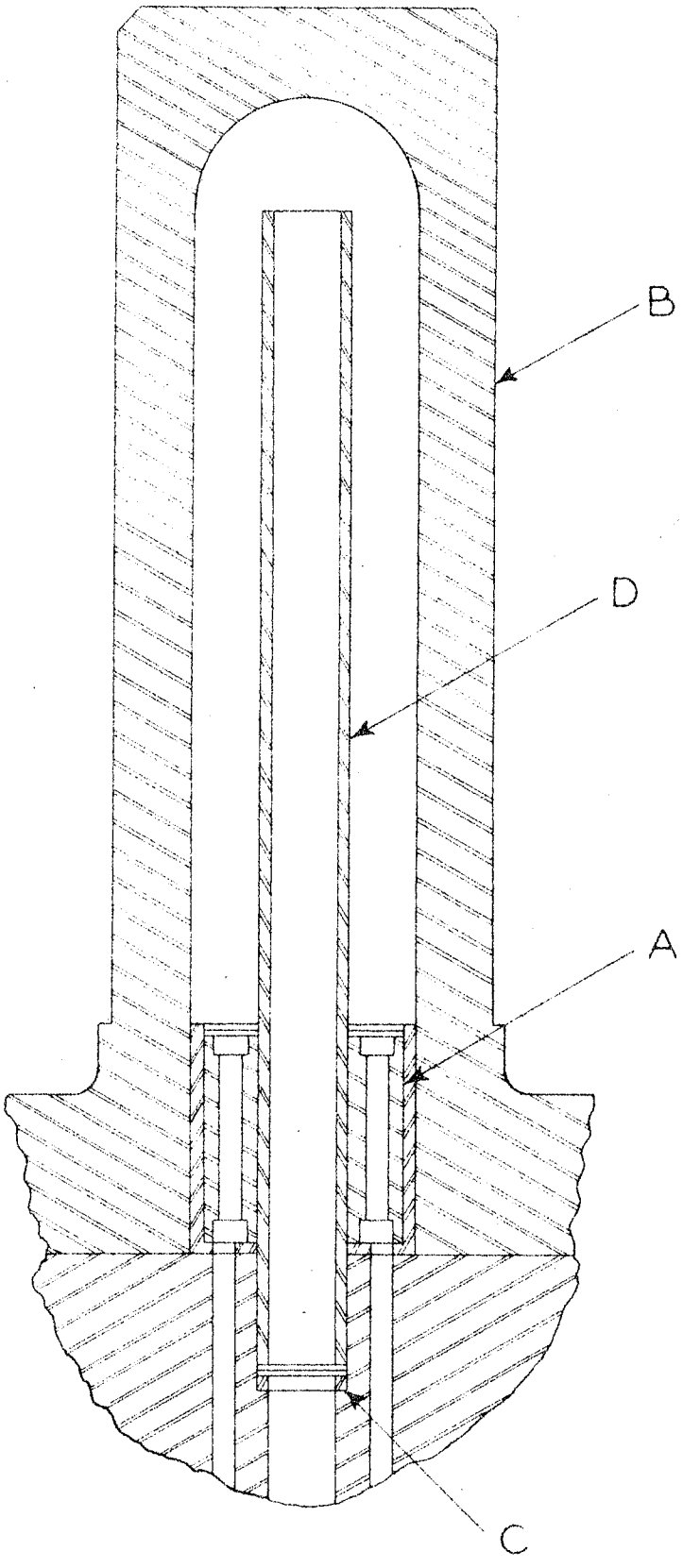

Fig. 1. Sectional View of Thimble Showing Supports for Silica Crystals

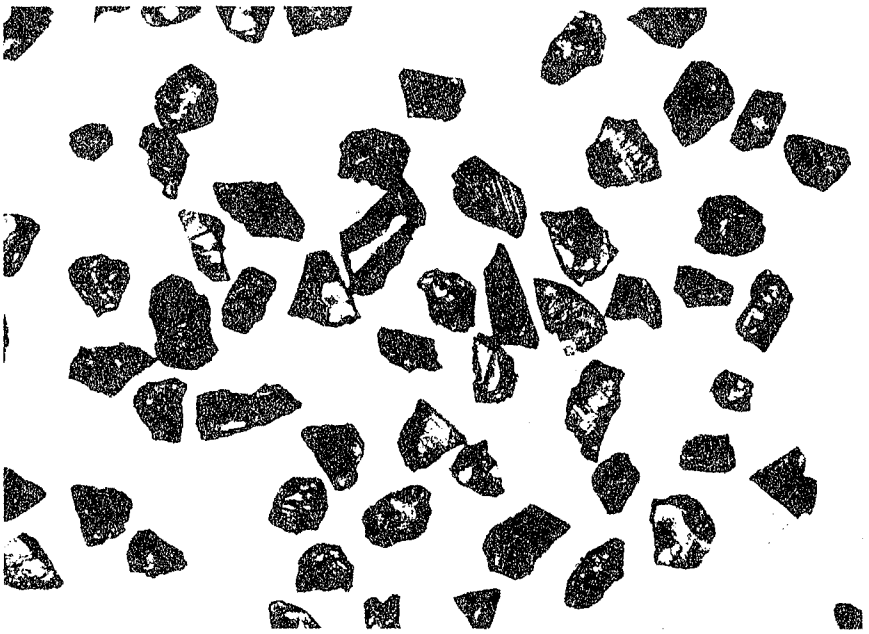

Fig. 2. Silica Crystals Magnified 23 Times

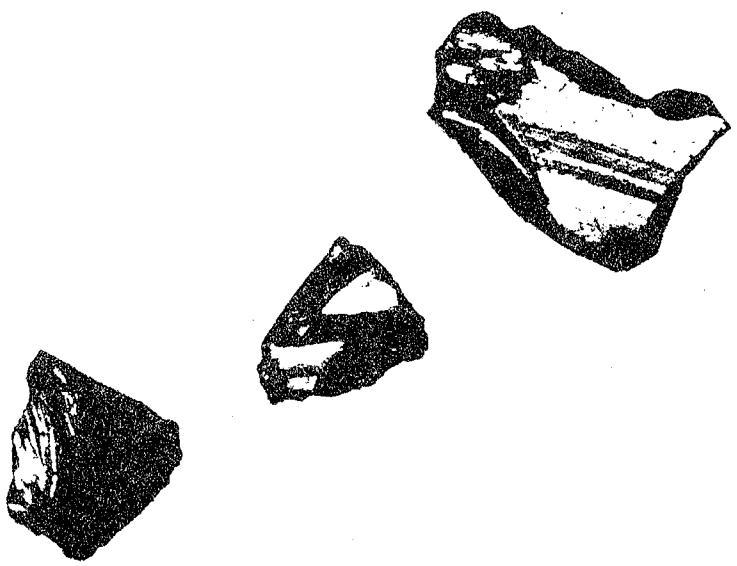

Fig. 3. Silica Crystals Magnified 70 Times

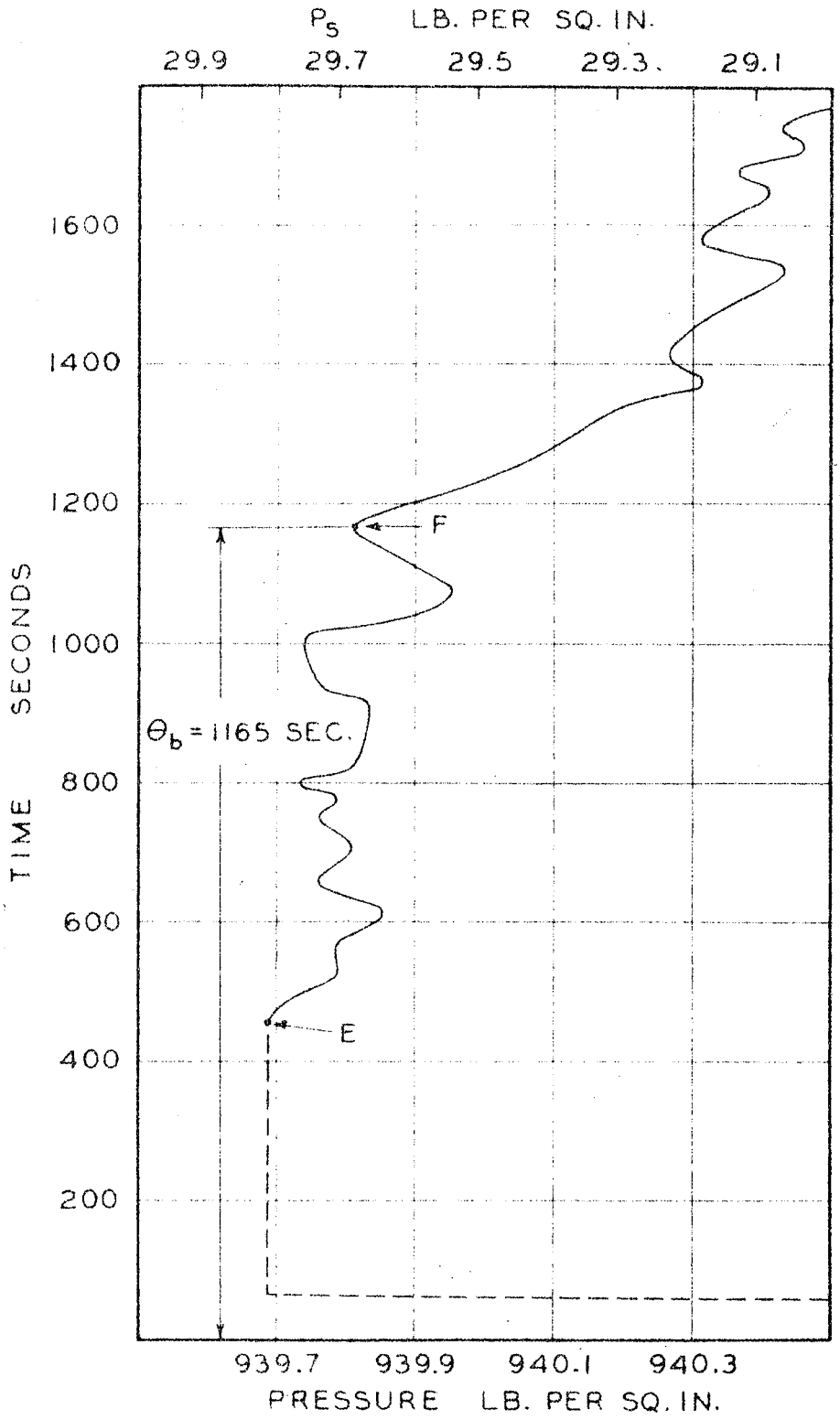

Fig. 4. Typical Results of Pressure-Time Measurements

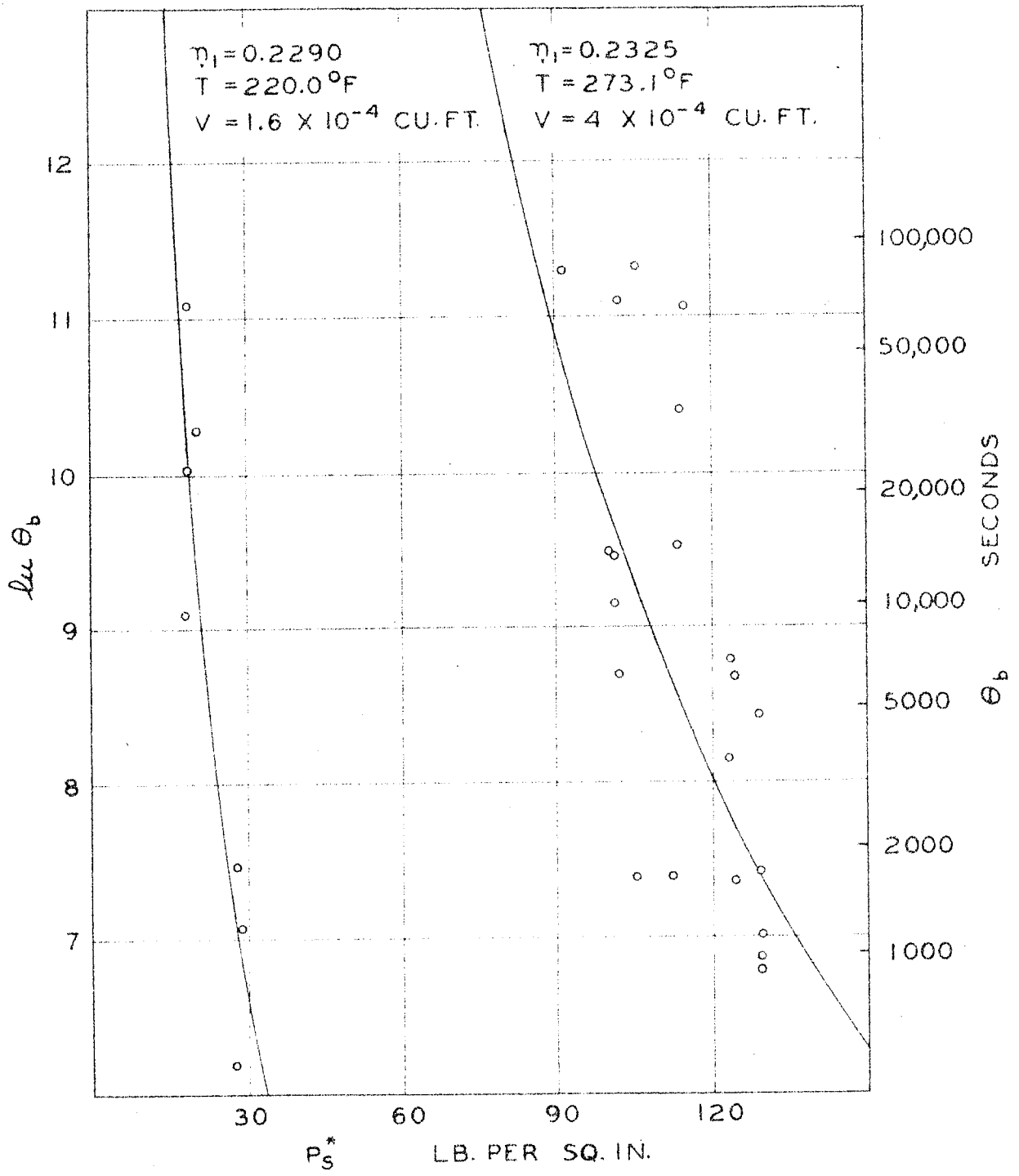

Fig. 5. Effect of Silica Crystals on Obtainable Degree of Supersaturation

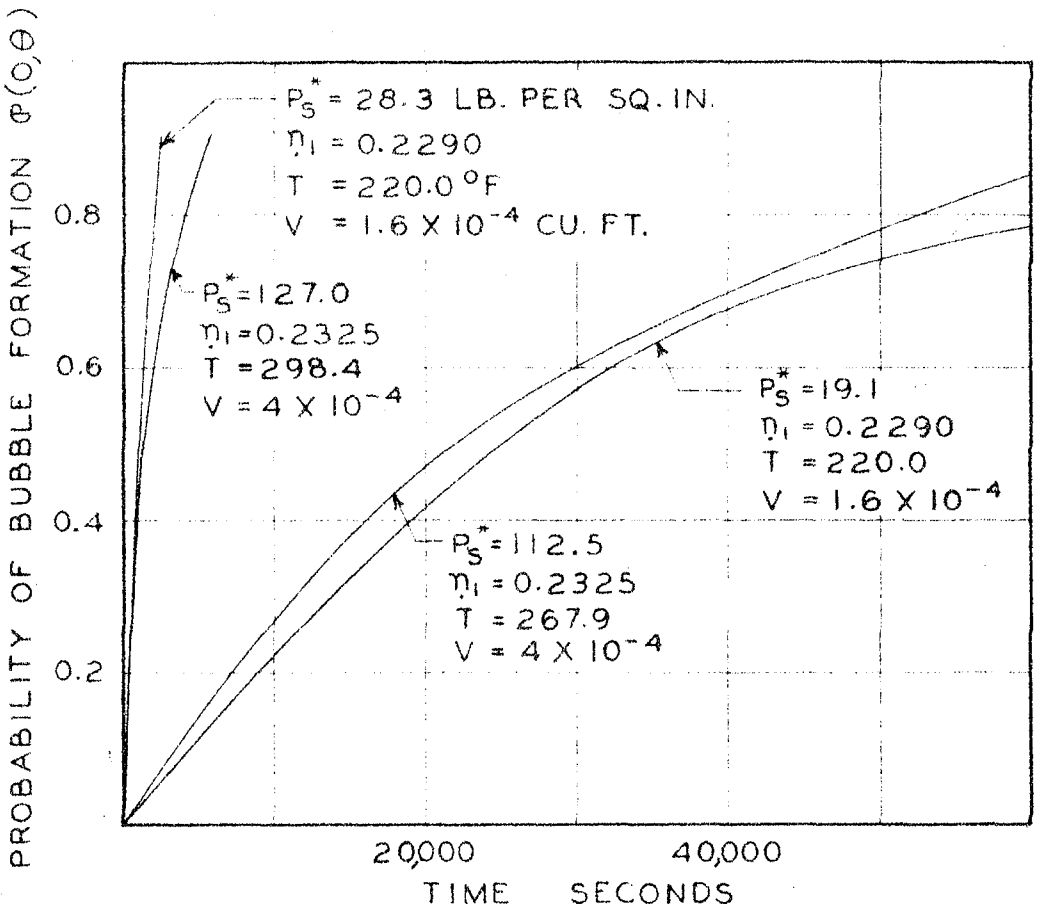

Fig. 6. Effect of Volume on the Probability of Bubble Formation

APPENDICES

APPENDIX A

THE MOLECULAR THEORY OF LIQUIDS

The rigorous theories of the liquid state are based on the evaluation of the partition function (5)

$$Z = \lambda^{-3N} \frac{1}{N!} \int e^{-\beta \Phi} \, dr_1, \cdots, dr_N .$$

Here, $\beta = 1/kT$; the first factor λ^{-3N} , with $\lambda = h/(2\pi m kT)^{1/2}$ is the result of the integration over the kinetic energy in the classical theory; the factor $1/N!$ is introduced because in the integration over all possible configurations with potential energies $\Phi(r_1,\cdots,r_N)$, configurations which differ only by a mere permutation of the molecules are counted as different "states" whereas they should be counted as identical states in the partition function.

The theoretical treatments of the liquid state are always based on the following assumptions about $\Phi(r_1,\cdots,r_N)$: (1) between every pair of molecules at a mutual distance r , there acts the same central force derived from the intermolecular potential field $\phi(r)$; (2) the total potential energy Φ is built up additively out of the contributions of the pairs of molecules, so that $\Phi(r_1,\cdots,r_N) = \sum\sum \phi(r)$. The potential field $\phi(r)$ is assumed to have the form

$$\phi(r) = 4\epsilon \left[(\sigma/r)^{12} - (\sigma/r)^{6} \right]$$

in which ϵ and δ are two quantities of the dimensions of an energy and a length respectively, which determine the magnitude of the intermolecular force and which may vary from substance to substance. These quantities ϵ and δ may be used to define molecular units for molar volume $(N\delta^3)$, energy $(N\epsilon)$, temperature $(N\epsilon/R = \epsilon/k)$ and pressure $(N\epsilon/N\delta^3 = \epsilon/\delta^3)$ where N equals the number of molecules.

The first attempts to give a description of liquids with the free-volume concept were made by Eyring (7) and Eyring and Hirschfelder (8), who used this concept to correlate the properties of liquids. Lennard-Jones and Devonshire (14) used the free-volume concept to explain the liquid properties in terms of the intermolecular forces. Since the more recent attempts to explain the properties of the liquid state are extensions or modifications of the theory of Lennard-Jones and Devonshire, the assumptions and principles of the theory are presented as a basis for further discussion.

The assumptions of this theory are:

(1) Each molecule is considered to be confined to a cell composed of its nearest neighbors. Exchange of molecules between cells is ignored. The partition function of the whole assembly is, therefore, the product of the N individual partition functions.

(2) Each cell is occupied. Its volume is $v = V/N$. The exact shape of the cell should be fixed by defining it as that part of space

which lies nearer to the central molecule than to any other, but for practical purposes each cell is taken to be a sphere. If the lattice sites form a face centered cubic structure, the volume of this sphere is $a^3/\sqrt{2}$, where a is the distance between lattice sites. The number of nearest neighbors, n, to each lattice site is 12 for such a structure.

(3) The potential energy inside each sphere is assumed to be spherically symmetrical. It is found by averaging over all angles the potential energy due to 12 molecules at distance a. There are two approximations involved here: first, the assumption of symmetry, and secondly, the assumption that all neighbors are at distance a.

The mean energy of a molecule at a distance x from the center of its cell, due to one neighbor at distance a from this center is given by

$$\bar{E}(x) = \frac{1}{2}\int_0^{\pi} E\left[\left(x^2 + a^2 - 2ax\cdot\cos\theta\right)^{1/2}\right]\cdot\sin\theta\, d\theta$$

If n molecules surround each lattice site, then the mean energy of the central molecule is given by

$$n\left[\bar{E}(x) - E(0)\right] = n\epsilon\left[q^{-4}\cdot\ell(y) - 2q^{-2}\cdot n(y)\right]$$

Here, $nE(0)$ is the energy at the center of the cell. On the right hand side, q is the reduced volume of the cell given (for $n = 12$) by

$$q = a^3/r_0^3\sqrt{12}$$

where, $$y = x^2/a^2$$

and $$\ell(y) = (1 + 12y + 25.2y^2 + 12y^3 + y^4)(1-y)^{-10} - 1$$

$$n(y) = (1+y)(1-y)^{-4} - 1$$

A "free-volume" $j(0)$ may be defined by

$$j(0) = 2\pi a^3 \cdot g = \int \exp\left\{-n\left[\bar{E}(x) - E(0)\right]/kT\right\} \cdot dr$$

or

$$g = \int_0^s y^{1/2} \cdot \exp\left\{-\frac{n\epsilon}{kT}\left[q^{-4} \cdot \ell(y) - 2q^{-2} \cdot n(y)\right]\right\} \cdot dy$$

in which for a face-centered lattice,

$$s = (3/4\pi\sqrt{2})^{2/3} = 0.30544$$

At infinite temperature $j(0)$ is $a^3/\sqrt{2}$, the volume of the cell. At finite temperature $j(0)$ is smaller than this, as each part of the cell is weighted with the approximate Boltzman factor.

The partition function of a single molecule is given by

$$f = (2\pi m k T/h^2)^{3/2} \cdot 2\pi a^3 \cdot q \cdot \exp\left[-n E(0)/2 k T\right]$$

The free energy and other thermodynamic functions may be expressed in terms of the partition function of the whole assembly, $Z = e^N \cdot f^N$. Here, a communal entropy term, e^N , is arbitrarily included.

The simple theory as first presented by Lennard-Jones and Devonshire gives a good qualitative explanation of the behavior of the liquid state. The fact that the entire volume of the liquid is not available to each molecule is probably of little importance at high densities; however, in the limit of low densities it means that the partition function is too low by a factor of $N!/N^N \approx e^{-N}$. The free energy is too high by RT. This may be accounted for by inserting an extra factor of e^N in the partition function. However, this is not very satisfactory, since the factor of e^N is needed in the perfect gas limit, but not in the perfect crystal. Somewhere between these limits it must become effective. Hirschfelder, Stevenson, and Eyring (11) took the view that it appears discontinuously at the melting point, where it contributes an extra amount of entropy, R, to the liquid. They called this term the "communal entropy". Rice (21) criticized this assumption and maintained the factor appeared more gradually. This would make it a function of volume as

well as temperature and so would cause it to contribute to the equation of state.

Since its inception, the Lennard-Jones and Devonshire theory has been used by numerous authors as a basis for additional investigations directed toward the development of a more quantitative description of the properties of the liquid state. Cernushi and Eyring (4) determined the distribution of molecules among the cells by the quasi-chemical approximation (9). However, they did not consider the effect of vacant cells on the partition of the individual molecule within its cell.

The effect of vacant sites around one lattice site, or "hole theory" as it has been called, upon the intermolecular potential has been analyzed by Ono (16), Peek and Hill (17), and Rowlinson and Curtiss (22). In general, the critical constants obtained by their methods are in somewhat better agreement with experimental results than those of the simple cell theory. The "hole theory" approximations give good results at the extremes of high and low densities, but need not be very good in between.

A more formal development was given by Kirkwood (13) and elaborated by Mayer and Careri (15). In the Kirkwood theory, the Gibbs configuration integral (10) is expressed as a sum of integrals corresponding to single and multiple occupancy of cells of a reference lattice. The integral corresponding to single occupancy is evaluated

with a probability density which may be approximated by a function depending only on the position of the molecule in its cell. The minimization of the free energy gives an integral equation for the probability density within each cell of the lattice. A first approximation of the solution of these equations yields a partition function identical with that of the Lennard-Jones and Devonshire theory. At best, the solutions of the integral equations are numerically difficult, and in all cases must be solved subject to an approximation which is sometimes called the variation principle. However, even the best trial function when used in the variation procedure gives a result for the free energy which is considerably too high.

Recently, Barker (1, 2) and de Boer (6) described independent methods for basing a formally convergent theory on the cell concept. The formal development is based on the idea of expanding the Gibbs integral (10) in a series of similar form to the virial series, with the first term corresponding to the simple theory, and with higher terms taking account of communal and coupling effects. The higher terms are not unduly large; thus, the cell theory provides a good first approximation to an exact theory. Unfortunately, only limited numerical values of the integrals required in these theories are presently available, however, the work of Barker appears to give better results than those of de Boer.

With the theory of the liquid state fairly well defined, several workers have attempted to expand the Lennard-Jones and Devonshire theory to describe more complex configurations than those covered by the simple cell theory. Applying the cell method to liquid mixtures, Prigogine and Methot (18) have developed a new theory for binary solutions relating all thermodynamic properties to molecular interactions. It is assumed that: the constituents are spherical in shape, with an isotropic field of force; the distance of the maximum interaction for all types of pairs of molecules is about the same; there is random mixing; and the mean potential field is of the smoothed potential type. Using the method of moments (12), Salsburg and Kirkwood (23) have extended the theory of the liquid state to multicomponent mixtures. Retention of only the first moment yields an approximation to the partition function recently studied by Prigogine and Methot (18).

An important step toward extending the molecular theory to chain molecules was taken by Prigogine, Trappeniers and Mathot (19) who derived expressions for one-component systems as well as mixtures. The approximations used to extend the simple cell theory to chain molecules are: the chain molecule is built up of identical centers with customary 6-12 interaction potential; the intermolecular field exerted on a repeating unit is approximated by a combination of a harmonic oscillator field with a volume-dependent frequency and a rigid sphere

repulsion; the difference between intra- and inter-molecular distances is disregarded and the quasi-crystalline lattice is characterized by a single lattice parameter; and internal rotations are unrestricted. Solutions of short chain molecules and high polymers have been discussed in terms of this theory by Bellemans and Colin-Naar (3) and Prigogine and Bellemans (20) respectively.

The cell theory in the formulation for chain type molecules was applied to normal paraffins, polyethylene and polystyrene by Simha and Hadden (24). Comparison of the theory with experimental data showed deviations of 10 to 20 per cent for the normal paraffins and polyethylene. The results for polystyrene were less favorable; however, their findings justify extending the theory to handle a wider range of variables, and other types of molecules.

While there are still numerous problems to resolve, great strides have been made since the cell theory was first proposed in 1937. With the intense interest in this field and the development of more advanced computational procedures and equipment, it is very probable that a nearly exact theory of the liquid state will be forthcoming in the near future.

REFERENCES

1. Barker, J. A., Proc. Roy. Soc., (London) A230, 390 (1955).

2. Barker, J. A., Proc. Roy. Soc., (London) A237, 63 (1956).

3. Bellemans, A., and Colin-Naar, C., J. Poly. Sci., 15, 121 (1955).

4. Cernushi, F., and Eyring, H., J. Chem. Phys., 7, 547 (1939).

5. de Boer, J., Proc. Roy. Soc. (London) A215, 4 (1952).

6. de Boer, J., Physica, 20, 655 (1954).

7. Eyring, H., J. Chem. Phys., 4, 283 (1936).

8. Eyring, H., and Hirschfelder, J., J. Phys. Chem., 41, 249 (1937).

9. Fowler, R. H., and Guggenheim, E. A., "Statistical Thermodynamics," Cambridge University Press, London, 1939.

10. Gibbs, J. W., "Collected Works," Vol. II, Longmans Green and Co., New York, 1931.

11. Hirschfelder, J., Stevenson, D., and Eyring, H., J. Chem. Phys., 5, 896 (1937).

12. Kirkwood, J. G., J. Chem. Phys., 6, 70 (1938).

13. Kirkwood, J. G., J. Chem. Phys., 18, 380 (1950).

14. Lennard-Jones, J. E., and Devonshire, A. F., Proc. Roy. Soc., (London) A163, 63 (1937).

15. Mayer, J. E., and Careri, G., J. Chem. Phys., 20, 1001 (1952).

16. Ono, S., "Memoirs of the Faculty of Engineering," Kyushu University, 10, 195 (1947).

17. Peek, H. M., and Hill, T. L., J. Chem. Phys., 18, 1252 (1950).

18. Prigogine, I., and Mathot, V., J. Chem. Phys., 20, 49 (1952).

19. Prigogine, I., Trappeniers, N., and Mathot, V., J. Chem. Phys., 21, 559 (1953).

20. Prigogine, I., and Bellemans, A., J. Poly. Sci., 18, 147 (1955).

21. Rice, O. K., J. Chem. Phys., 6, 476 (1938).

22. Rowlinson, J. S., and Curtiss, C. F., J. Chem. Phys., 19, 1519 (1951).

23. Salsburg, Z. W., and Kirkwood, J. G., J. Chem. Phys., 20, 1538 (1952).

24. Simha, R., and Hadden, S. T., J. Chem. Phys., 25, 702 (1956).

NOMENCLATURE

a	distance between lattice sites
$\bar{E}$	mean energy of a molecule
f	partition function of a single molecule
g	integral related to the free volume
h	Planck constant
j(o)	free volume
k	Boltzman constant
m	mass of molecule
n	number of molecules around one lattice site
N	total number of molecules
q	reduced cell volume
r	distance between a pair of molecules
r_o	distance characteristic of the intermolecular potential
R	universal gas constant
T	absolute temperature
v	volume per molecule
V	volume per mole
x	distance from molecule to center of cell
Z	partition function of entire lattice assembly
ϵ	energy characteristic of the intermolecular potential
$\phi(r)$	intermolecular potential field

Φ total potential energy

δ collision diameter

APPENDIX B

STATISTICAL PROCEDURES FOR SUPERSATURATION DATA

STATISTICS

For points distributed individually and collectively at random, the probability of n points lying within a certain interval is given by the Poisson distribution. In Poisson's distribution (1), the spectrum consists of all non-negative integers, and the distribution is given by:

$$\varphi_i = \frac{\lambda^i}{i!} \cdot e^{-\lambda} \tag{1}$$

where $\lambda > 0$

and $i = 0, 1, 2, \cdots$

$$\sum_{i=0}^{\infty} \varphi_i = e^{-\lambda} \sum_{i=0}^{\infty} \frac{\lambda}{i!} = e^{-\lambda} e^{\lambda} \equiv 1 \tag{2}$$

where λ is a parameter.

Letting the random variable be the number of bubbles forming in the time interval from 0 to θ, and assuming that: (a) the probability of a bubble forming in the time $d(0,\theta)$ is $k\, d(0,\theta)$, and (b) the bubble formations are independent; then the random variable is Poisson distributed. Denoting the probability of n bubbles in the time 0 to θ by $\varphi_n(0,\theta)$, then $\varphi_n\left[(0,\theta) + d(0,\theta)\right]$ is equal to the product of the probabilities of n bubbles in 0 to θ and no bubbles in $d(0,\theta)$ plus the product of the probabilities of n-1 bubbles in 0 to θ and

one in $d(0,\theta)$. Since $d(0,\theta)$ is a differential, the probability of more than one bubble in $d(0,\theta)$ is of higher order and therefore negligible. Thus, from the assumptions (1) we have:

$$P_n\left[(0,\theta) + d(0,\theta)\right] = P_n(0,\theta)\left[1 - k\,d(0,\theta)\right] + P_{n-1}(0,\theta)\,k\,d(0,\theta) \tag{3}$$

from which

$$\frac{dP_n(0,\theta)}{d(0,\theta)} = k\left[P_{n-1}(0,\theta) - P_n(0,\theta)\right] \tag{4}$$

The solution of this infinite system of differential equations is uniquely given by Poisson's formula, with $\lambda = k\theta$.

$$P_n(0,\theta) = \frac{(k\theta)^n}{n!}\, e^{-k\theta} \tag{5}$$

where $k\theta$ is the expected number of bubbles formed within the time interval. The probability of no bubbles forming in the interval from 0 to θ may be established from

$$P_0(0,\theta) = e^{-k\theta} \tag{6}$$

The probability of no bubbles forming up to θ, as given by Equation 6, is equal to the probability of the first bubble forming at some time later than θ, and so

$$e^{-k\theta} = \int_0^{\infty} f(\theta)\,d\theta = 1 - \int_0^{\theta} f(\theta)\,d\theta \tag{7}$$

where $f(\theta)$ is the distribution function of times for the first bubble to form. Upon differentiation, Equation 7 yields

$$f(\theta) = k e^{-k\theta} \tag{8}$$

The mean time for the first bubble to form is given by

$$\bar{\theta} = \int_0^\infty \theta f(\theta)\, d\theta = \int_0^\infty k\theta\, e^{-k\theta} d\theta = \frac{1}{k} \tag{9}$$

The variance is

$$\begin{aligned} \delta^2 &= \int_0^\infty (\theta-\bar{\theta})^2 f(\theta) d\theta = \int_0^\infty (\theta^2 - 2\theta\bar{\theta} + \bar{\theta}^2) f(\theta)\, d\theta \\ &= k(2/k^3) + 1/k^2 - 2/k^2 = 1/k^2 \end{aligned} \tag{10}$$

The standard deviation is therefore

$$\delta = \frac{1}{k} \tag{11}$$

Under circumstances in which the first bubble formation does not effect the formation of subsequent bubbles, the reciprocal of the mean time for the first bubble to form is the rate of bubble formation for the given volume.

$$\mathring{n}_b = \frac{1}{\bar{\theta}} = k \tag{12}$$

If the bubble forms at random throughout the entire sample, a rate of bubble formation per unit volume may be calculated. The probability of no bubbles forming in the interval from 0 to θ is given by Equation 6; thus, the probability of the first bubble forming in this interval must be

$$P(0,\theta) = 1 - e^{-k\theta} = 1 - e^{-\mathring{n}_b\theta} \tag{13}$$

which upon rearrangement yields

$$\ln\left[1 - P(0,\theta)\right] = -\mathring{n}_b\theta \tag{14}$$

In accordance with Equation 14, a plot of $\ln\left[1-P(0,\theta)\right]$ versus θ should yield a straight line with a slope equal to the negative reciprocal of the mean time.

The rate of bubble formation may be approximated by the Arrhenius equation

$$\mathring{n}_b = A\, e^{-\underline{w}/bT} \tag{15}$$

The work, $\underline{w}$, necessary to form a bubble of critical size has the appearance of an activation energy. An expression for this work has been derived by Gibbs (2).

$$\underline{w} = \frac{16\pi\gamma^3}{3bT(P_b - P)^2} \tag{16}$$

Combination and rearrangement of Equations 15 and 16 yields the expression

$$\ell n\, \mathring{n}_b - \ell n\, A = - \frac{16\pi\gamma^3}{3bT(P_b-P)^2} \tag{17}$$

or, applying Equation 12, Equation 17 can be written as

$$\ell n\, \bar{\theta}_b + \ell n\, A = \frac{\alpha}{(P_b-P)^2} \tag{18}$$

Because the supersaturation pressure could not be held exactly throughout the duration of an experimental test, Equation 18 was used to adjust the data to a uniform degree of supersaturation. For small adjustments of the order of one or two pounds per square inch, Equation 18 should be satisfactory; although its validity over a much larger range has not been investigated.

REGRESSION ANALYSIS

In determining the numerical value of the constant α in Equation 18, the following hypothesis was proposed:

$$\ell n\, \frac{\mu_i}{a} = \frac{\alpha}{S_i^2} \quad ; \quad \mu_i = a\, e^{\alpha/S_i^2} \tag{19}$$

where S_i has been written for the supersaturation pressure $P_b - P$ and μ_i for the $\bar{\theta}$ corresponding to $P_b - P$. The distribution function

may be put in the form

$$f(t_i) = \frac{1}{\mu_i} e^{-t_i/\mu_i} \tag{20}$$

in which the time for the first bubble to form is denoted by t_i . Substitution of Equation 19 into Equation 20 yields the expression

$$f(t_i) = \frac{1}{a} e^{-\alpha S_i^{-2}} e^{-(\frac{1}{a} t_i e^{-\alpha S_i^{-2}})} \tag{21}$$

The likelihood (3) is written as

$$L = \prod_{i=1}^{n} \frac{1}{a} e^{-\alpha S_i^{-2}} e^{-(\frac{1}{a} t_i e^{-\alpha S_i^{-2}})} \tag{22}$$

Since the logarithm of the likelihood has its maximum at the same point as does the likelihood, the logarithm is used because it is simpler to maximize.

$$\ell n\, L = \sum_{i=1}^{n} \left[(-\alpha S_i^{-2}) - \ell n\, a - \frac{1}{a} t_i e^{-\alpha S_i^{-2}} \right] \tag{23}$$

$$= -\sum_{i=1}^{n} \alpha S_i^{-2} - n\, \ell n\, a - \frac{1}{a} \sum_{i=1}^{n} t_i e^{-\alpha S_i^{-2}}$$

By differentiating Equation 23 separately with respect to a and α and setting both derivatives equal to zero, the maximum may be located.

$$\frac{\partial \ell n L}{\partial a} = -\frac{n}{a} + \frac{1}{a^2}\sum_{i=1}^{n} t_i e^{-\alpha S_i^{-2}} = 0 \tag{24}$$

Solving for a

$$a = \frac{1}{n}\sum_{i=1}^{n} t_i e^{-\alpha S_i^{-2}} \tag{25}$$

$$\frac{\partial \ell n L}{\partial \alpha} = -\sum_{i=1}^{n} S_i^{-2} + \frac{1}{a}\sum_{i=1}^{n} t_i S_i^{-2} e^{-\alpha S_i^{-2}} = 0 \tag{26}$$

$$a\sum_{i=1}^{n} S_i^{-2} = \sum_{i=1}^{n} t_i S_i^{-2} e^{-\alpha S_i^{-2}} \tag{27}$$

A combination of Equations 25 and 27 results in

$$\sum_{i=1}^{n} t_i S_i^{-2} e^{-\alpha S_i^{-2}} = \frac{1}{n}\left[\sum_{i=1}^{n} t_i e^{-\alpha S_i^{-2}}\right]\left[\sum_{i=1}^{n} S_i^{-2}\right] \tag{28}$$

Equation 28 must be solved by a lengthy trial and error procedure. Rearrangement of Equation 28 gives

$$1 - \frac{\sum_{i=1}^{n} t_i S_i^{-2} e^{-\alpha S_i^{-2}}}{\frac{1}{n}\left[\sum_{i=1}^{n} t_i e^{-\alpha S_i^{-2}}\right]\left[\sum_{i=1}^{n} S_i^{-2}\right]} = 0 \qquad (29)$$

By plotting the right hand side of Equation 29 versus α, a nearly straight line is obtained; which reduces the amount of computation necessary to fix the value of α.

The author is indebted to W. B. Nichols who developed the statistical procedures for the supersaturation data as presented here and used to adjust the data in Part I of this thesis.

REFERENCES

1. Arley, N., and Buch, K. R., "Introduction to the Theory of Probability and Statistics," John Wiley and Sons, Inc., New York, 1953.

2. Gibbs, J. W., "Collected Works," Vol. I, Longmans Green and Co., New York, 1931.

3. Mood, A. M., "Introduction to the Theory of Statistics," McGraw-Hill Book Co., Inc., New York, 1950.

NOMENCLATURE

a	reciprocal of A
A	frequency factor in Arrhenius rate equation
b	specific gas constant
$f(\theta)$	distribution function of times for first bubble to form
i	running index
k	parameter in Poisson distribution
L	likelihood function
n	number of sample points, the nth sample point
n_b	rate of bubble formation
P	pressure
P_b	bubble-point pressure
φ	probability
φ_n	probability of n bubbles being formed
φ_{n-1}	probability of n-1 bubbles being formed
φ_o	probability of no bubbles being formed
S_i	degree of supersaturation (P_b-P) for ith sample point
t_i	time for first bubble to form for ith sample point
T	absolute temperature
w	work necessary to form bubble of critical size
α	$16\pi\gamma^3/3bT$
γ	interfacial tension, lb./ft.

θ time for first bubble to form

$\bar{\theta}$ population mean of times for the first bubble to form

$\bar{\theta}_b$ sample mean of times for the first bubble to form

λ_i parameter in Poisson distribution

μ_i mean time corresponding to S_i

δ standard deviation

φ_i spectrum in Poisson distribution